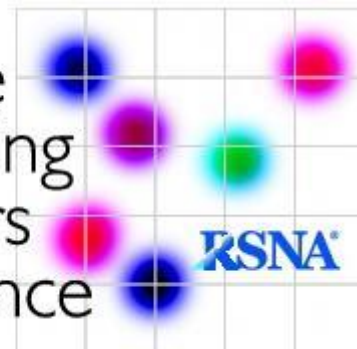


Quantitative
Imaging
Biomarkers
Alliance



QIBA Profile:

Diffusion-Weighted Magnetic Resonance
Imaging (DWI)

1
2
3
4
5

		Table of Contents	
6			
7	Change Log:		4
8	Open Issues:		5
9	Closed Issues:		6
10	1. Executive Summary		8
11	2. Clinical Context and Claims		9
12	2.1 Clinical Context		9
13	2.2 Claims		9
14	2.3 Clinical Interpretation		11
15	3. Profile Activities		12
16	3.1. Staff Qualification		13
17	3.1.1 Discussion		13
18	3.1.2 Specification		14
19	3.2. Site qualification		14
20	3.2.1 Discussion		14
21	3.2.2 Specification		15
22	3.3. Pre-delivery		16
23	3.3.1 Discussion		17
24	3.3.2 Specification		17
25	3.4. Installation		17
26	3.5. Periodic QA		17
27	3.5.1 Discussion		17
28	3.5.2 Specification		17
29	3.6. Protocol Design		17
30	3.6.1 Discussion		18
31	3.6.2 Specification		18
32	3.6.2.1 Brain		19
33	3.6.2.2 Liver		20
34	3.6.2.3 Prostate		21
35	3.6.2.4 Breast		23
36	3.7. Subject Selection		24
37	3.7.1 Discussion		24
38	3.8. Subject Handling		24
39	3.8.1 Discussion		24
40	3.9. Image Data Acquisition		24

41	3.9.1 Discussion	25
42	3.9.2 Specification	25
43	3.10. Image Data Reconstruction	25
44	3.10.1 Discussion	25
45	3.10.2 Specification	26
46	3.11. Image QA	26
47	3.11.1 Discussion	26
48	3.11.2 Specification	32
49	3.12. Image Distribution	32
50	3.12.1 Discussion	32
51	3.12.2 Specification	33
52	3.13. Image Analysis	33
53	3.13.1 Discussion	33
54	3.13.1.1 Brain	34
55	3.13.1.2 Liver	34
56	3.13.1.3 Prostate	34
57	3.13.1.4 Breast	34
58	3.13.2 Specification	34
59	4. Assessment Procedures	36
60	4.1. Assessment Procedure: ADC bias and precision	36
61	4.2. Assessment Procedure: Voxel SNR	36
62	4.3. Assessment Procedure: ADC <i>b</i> -value Dependence	37
63	4.4. Assessment Procedure: ADC Spatial Bias	37
64	4.5. Assessment Procedure: Image Analysis Software	37
65	References	39
66	Appendices	45
67	Appendix A: Acknowledgements and Attributions	45
68	Appendix B: Background Information	46
69	Appendix C: Conventions and Definitions	47
70	Appendix D: Platform-Specific Acquisition Parameters for DWI Phantom Scans	48
71	Appendix E: Technical System Performance Evaluation	52
72	E.1. ADC Qualities at/near Isocenter	52
73	E.2. DWI Signal to Noise	54
74	E.3. ADC <i>b</i> -value dependence	56
75	E.4. ADC Spatial Dependence	57

76	Appendix F: Checklists	58
77	F.1. Site Checklist	58
78	F.2. Acquisition Device Checklist	59
79	F.3. Scanner Operator Checklist	61
80	F.4. Image Analyst Checklist	64
81	F.5. Reconstruction Software	66
82	F.6. Image Analysis Tool Checklist	67

83

84 Change Log:

85 This table is a best-effort of the authors to summarize significant changes to the Profile.

Date	Sections Affected	Summary of Change
2015.10.10	All	Major cleanup based on comments resolved in the Process Cmte. Also had to remove a few hundred extraneous paragraph styles.
2015.10.21	All	Approved by Process Cmte
2015.11.04	2 (Claims) 3 (Requirements)	Incorporating the more refined form of the claim language and referenced a separate claim template. Added Voxel Noise requirement to show example of the linkage between the requirement and the assessment procedure.
2015.12.16		Minor changes to remove reference to "qualitative" measurements, fix reference to guidance and clean some formatting.
2016.01.06	1, 3.8.1	Rewording to avoid the term "accuracy".
2016.11.21	2	Removed polygonal brain ROI area reference (not literature-supported)
2017.01.18	All	Endnote library of references, prostate added, reconciled ToC with actual content, fixed formatting, cleaned up most comments and highlights, ready for PDF review
2017.10.26	Section 3	Added new 3.6x (protocol design) and moved organ-specific scan protocols there
2017.11.02	Section 3	Added new subsections 3.0x, 3.1x, 3.2x to comply with 07.2017 template
2017.11.14	Sections 2,3,4	Rearranged material from Appendix E and section 4 between new subsections in 3 and 4, and added subsection 2.1 (clinical interpretation)
2017.11.15	Section 4	Shortened and bulleted the assessment procedure for phantom
2017.11.16	Section 3	Updated phantom study refs to include Pierpaoli and Palacios
2018.07.24	Section 3	Removed redundant text in all activities (esp. 3.13), removed 3.14
2018.07.26	Section 3, Table 1	Combined activities and sections on one line for some actors
2018.07.27	Section 3	Reconciled discussion and spec tables for all activities (esp.3.2.2)
2018.07.30	Section 3.11	Added artefact examples
2019.01.16	Appendix F	Added checklists, standardized format
2019.01.16	2 (claims), 3	Added breast specs to profile, per 6698 test-retest data, call outs to references (added these to endnote library, need to be in-line cited)
2019.01.18	All	Artifact and derivatives all changed to "artefact"

2019.01.18	3.6.2, 3.13.2	Created new heading format (heading 4) for organ-specific specs and image artefact discussion.
2019.01.30	All	Accepted changes from 2019.01.23 version. Removed references to Spick. Deleted old comments previously addressed.
2019.01.30	3.11	Resized Figure 4, changed caption to appear on right-hand side
2019.01.30	2.1	<i>Deleted Comment:</i> We either: Remove 56-58 since non-stats & only prostate. Or: Add all other test-retest papers used in claims & can include Spick, Koreans, Alui References added per call outs in above bullet point for each disease site.
2019.01.30	3.6.2.4	Ideal/target channels 5-16, acceptable 4 channels Number of <i>b</i> -values Ideal 4, target/acceptable 3 Gap thickness acceptable left at 1 mm per 6698 spec (all gaps 0 in study) Slice thickness ideal 4, target 4-5, acceptable 5 mm (not ≤ 4 because may affect SNR) NSA I/T:3-5, A:2 TE Ideal/target: min TE (50-100), acceptable <114 ms
2019.02.01	All	Artifact and derivatives all changed to “artefact” (again)
2019.02.05	F.2, F.5,F.6,	Retained “Reconstruction Software” as an Actor, removed highlighting. Created new Actor checklist for Recon S/W (F.5), moving specifications from F.2 matching those in 3.2. Image Analysis Tool Checklist renumbered to F.6.
2019.02.05	3.13.1.4	Added text to breast discussion
2019.02.05	2- Claims discussion	Adjusted text to include breast and claims for the same.
2019.02.05	3.6.2, F.2	Added Acquisition Device to 3.6.2 organ-specific protocol Actors. Created Scan Protocol Parameters in Acq. Device Checklist
2019.10.14	All	Finished incorporating edits based on Public Comment 2 Feedback-summary found online

86

87 Open Issues:

88 The following issues are provided here to capture associated discussion, to focus the attention of
89 reviewers on topics needing feedback, and to track them so they are ultimately resolved. In particular,
90 comments on these issues are highly encouraged during the Public Comment stage.

Q: How to address subject repeatability conformance/assessment?
Q: Are heading formats consistent? Do they make sense? Are they aligned with latest profiles? (may be Process Cmte. question)
Q: Do spec tables need to be adjusted to match width of text? Should column margins be adjusted for optimal legibility?
Reference 100 may needs reformatting (adjusted in EndNote entry, not reflecting in word document) to avoid linebreak (EF Jackson, AAPM report ref)
Q: Will the Profile address the use of DWI at high (e.g., >3 T) and low (<1.5 T) field strengths?

91 **Closed Issues:**

92 The following issues have been considered closed by the biomarker committee. They are provided here to
 93 forestall discussion of issues that have already been raised and resolved, and to provide a record of the
 94 rationale behind the resolution.

<p>Q. Which organs have sufficient reproducibility literature for inclusion in the longitudinal claim statement?</p> <p>A. Organs for inclusion are brain, liver, prostate, and breast. The following organs were considered, but have been excluded for the time being due to lack of sufficient literature (test-retest data from a total of ~35 subjects, either from a single publication or in total from multiple manuscripts) support: Bone, Kidney, Lymphoma, Pancreas, Head and neck, Lung, Whole Body</p>
<p>Q. How much of the Subject Handling subsection (3.1) is applicable to DWI?</p> <p>A. Text has been adjusted according to standard clinical practice, subject to public review</p>
<p>Q. Should organ-specific protocols be changed to the profile template’s table format, or left as-is?</p> <p>A. Protocols were adapted for the three organs discussed in the first DWI profile.</p>
<p>Q. Can references be better formatted?</p> <p>A. Now using EndNote Library in Word, not sure how this will translate to Google Docs.</p>
<p>Q. Who to include in Appendix B</p> <p>A. RSNA staff has provided current roster, this issue can be addressed in Google Docs while PDF is reviewing, with a final review at the BC level prior to handoff to MR CC.</p>
<p>Q. Comments in Prostate Section</p> <p>A. As the most recently edited organ section, we ask PDF readers to examine the claims and justifications prior to moving up to the MR CC level.</p>
<p>Q. How to make conformance section conform?</p> <p>A. Old “phantom” Conformance section moved mostly to Appendices, current structure reflects profile template from Process Committee</p>
<p>Q. What DICOM parameters should be specified in section 3.2.2?</p> <p>A. In public tags, vendors should provide: <i>b</i>-value; diffusion gradient direction (3-vector) or “isotropic”; sequence class (single spin-echo monopolar; single spin-echo bipolar; double spin-echo bipolar; stimulated echo); This was addressed, section is now 3.6</p>
<p>Q. Include images of relevant artefacts for Image QA section 3.8 (now 3.11)</p> <p>A. Artefacts added, captions written for all bullets in 3.11.1</p>
<p>Q. Need to edit 3.0 “site conformance” according to DWI workflow (or remove the subsection)?</p> <p>A. Added overall activity conformance and wCV test</p>
<p>Q. Need to reconcile spec-tables and discussion in new subsections 3.1.x and 3.2.x for DWI</p> <p>A. Focused discussion on profile activities for staff and site qualification</p>
<p>Q. Need to reconcile TOC w/new (added) subsections in 2 and 3 and changed headings in 4</p> <p>A. Reconciled during edits, must be recompiled anytime there are changes to section/subsection/subsubsection layout</p>
<p>Q. Need to update Table 1 and Figure 1 to include new actors/activities with the reference to correct subsections in 3</p> <p>A. Clarified figure title to point to key profile activities within trial workflow</p>
<p>Q: How to address ROI placement variability across radiologists?</p>

A: Potentially, use groundwork projects to assess the variability across radiologists from different sites, generate assessment procedures for the same.
Q: How to address breast protocol, particularly <i>b</i>-values? Need to adjust citations accordingly.
A: Newitt and Sorace used as primary citations. Target/acceptable reduced to 3 <i>b</i>-values
Q: Provide accessible link to DWI DRO (QIBA wiki)?
A: DRO and QIBAPhan software placed in publicly-accessible area of QIDW, short URLs adjusted accordingly and tested.
Q: What needs to go in <u>3.13.1.4 Breast</u>? <u>If nothing additional, 3.13.1.4 should be eliminated.</u>
A: Added text about avoiding potential bias sources in ROI selection.

96 **1. Executive Summary**

97 The goal of a QIBA Profile is to help achieve a useful level of performance for a given biomarker. The
98 **Claim** (Section 2) describes the biomarker performance and is derived from the body of scientific literature
99 meeting specific requirements, in particular test-retest studies. The **Activities** (Section 3) contribute to
100 generating the biomarker. Requirements are placed on the **Actors** that participate in those activities as
101 necessary to achieve the Claim. **Assessment Procedures** (Section 4) for evaluating specific requirements
102 are defined as needed to ensure acceptable performance.

103 Diffusion-Weighted Imaging (DWI) and the Apparent Diffusion Coefficient (ADC) are being used
104 clinically as qualitative (DWI) and quantitative (ADC) indicators of disease presence, progression or
105 response to treatment [1-29]. Use of ADC as a robust quantitative biomarker with finite confidence intervals
106 places additional requirements on Sites, Acquisition Devices and Protocols, Field Engineers, Scanner
107 Operators (MR Technologists, Radiologists, Physicists and other Scientists), Image Analysts,
108 Reconstruction Software and Image Analysis Tools [30-37]. Additionally, due to the intrinsic dependence
109 of measured ADC values on biophysical tissue properties, both the Profile Claims and the associated scan
110 protocols (Section 3.6.2) are organ-specific. All of these are considered **Actors** involved in **Activities** of
111 Acquisition Device Pre-delivery and Installation, Subject Handling, Image Data Acquisition,
112 Reconstruction, Registration, ADC map generation, Quality Assurance (QA), Distribution, Analysis, and
113 Interpretation. The requirements addressed in this Profile are focused on achieving ADC values with
114 minimal systematic bias and measurement variability [34, 36, 37].

115 **DISCLAIMER:** Technical performance of the MRI system can be assessed using a phantom having known
116 diffusion properties, such as the QIBA DWI phantom. The clinical performance target is to achieve a 95%
117 confidence interval for measurement of ADC with a variable precision depending on the organ being
118 imaged and assuming adequate technical performance requirements are met. While in vivo DWI/ADC
119 measurements have been performed throughout the human body, this Profile focused on four organ systems,
120 namely brain, liver, prostate, and breast as having high clinical utilization of ADC with a sufficient level of
121 statistical evidence to support the Profile Claims derived from the current peer-reviewed literature. In due
122 time, new DWI technologies with proven greater performance levels, as well as more organ systems will
123 be incorporated in future Profiles.

124 This document is intended to help a variety of users: clinicians using this biomarker to aid patient
125 management; imaging staff generating this biomarker; MRI system architects developing related products;
126 purchasers of such products; and investigators designing clinical trials utilizing quantitative diffusion-based
127 imaging endpoints.

128 Note that this document only states requirements specific to DWI to achieve the claim, not requirements
129 that pertain to clinical standard of care. Conforming to this Profile is secondary to proper patient care.

130 2. Clinical Context and Claims

131 2.1 Clinical Context

132 The goal of this profile is to facilitate appropriate use of quantitative diffusion weighted imaging (DWI) to
133 gain insight into changes in the microstructure and composition of lesions in humans using precise
134 quantitative measurements of the apparent diffusion coefficient (ADC) for robust tissue characterization
135 and longitudinal tumor monitoring. The premise for its use is that therapy-induced cellular necrosis should
136 pre-date macroscopic lesion size change, thereby motivating exploration of ADC as a response biomarker
137 [3, 5, 6, 13, 14, 16, 18, 19, 22, 26, 27, 38-40]. Within days to weeks after initiation of effective cytotoxic
138 therapy, tumor necrosis occurs, with a loss of cell membrane integrity and an increase of the extracellular
139 space typically resulting in a relative increase in ADC. During the following weeks to months, the tumor
140 may show shrinkage with a resorption of the free extracellular fluid and fibrotic conversion leading to a
141 decrease of the ADC, although tumor recurrence can also result in reduced ADC [21, 41, 42].

142
143 The objective of this Profile is to provide prerequisite knowledge of the expected level of variance in ADC
144 measurement unrelated to treatment, in order to properly interpret observed change in ADC following
145 treatment [30, 34, 36].

146
147 This QIBA DWI Profile makes Claims about the confidence with which ADC values and changes in a
148 lesion can be measured under a set of defined image acquisition, processing, and analysis conditions. It also
149 provides specifications that may be adopted by users and equipment developers to meet targeted levels of
150 clinical performance in identified settings. The intended audience of this document includes healthcare
151 professionals and all other stakeholders invested in the use of quantitative diffusion biomarkers for
152 treatment response and monitoring, including but not limited to:

- 153 • Radiologists, technologists, and physicists designing protocols for ADC measurement
- 154 • Radiologists, technologists, physicists, and administrators at healthcare institutions considering
155 specifications for procuring new MR equipment
- 156 • Technical staff of software and device manufacturers who create products for this purpose
- 157 • Biopharmaceutical companies and clinical trialists
- 158 • Clinicians engaged in therapy response monitoring
- 159 • Radiologists and other health care providers making quantitative measurements on ADC maps
- 160 • Oncologists, urologists, neurologists, other clinicians, regulators, professional societies, and others
161 making decisions based on quantitative diffusion image measurements
- 162 • Radiologists, health care providers, administrators and government officials developing and
163 implementing policies for brain, liver, prostate, and breast cancer treatment and monitoring

164 2.2 Claims

165 **Conformance to this Profile by all relevant staff and equipment supports the following claim(s):**

166 **Claim 1a: A measured change in the ADC of a brain lesion of 11% or larger indicates**
167 **that a true change has occurred with 95% confidence.**

168 **Claim 2a: A measured change in the ADC of a liver lesion of 26% or larger indicates**
169 **that a true change has occurred with 95% confidence.**

170 **Claim 3a:** A measured change in the ADC of a prostate lesion of 47% or larger
171 indicates that a true change has occurred with 95% confidence.

172 **Claim 4a:** A measured change in the ADC of a breast lesion of 13% or larger indicates
173 that a true change has occurred with 95% confidence.

174 -----

175 **Claim 1b:** A 95% CI for the true change in ADC of a brain lesion is given below, where
176 Y_1 and Y_2 are the ADC measurements at the two time points:

177
$$(Y_2 - Y_1) \pm 1.96 \times \sqrt{(Y_1 \times 0.040)^2 + (Y_2 \times 0.040)^2}.$$

178 **Claim 2b:** A 95% CI for the true change in ADC of a liver lesion is given below, where
179 Y_1 and Y_2 are the ADC measurements at the two time points:

180
$$(Y_2 - Y_1) \pm 1.96 \times \sqrt{(Y_1 \times 0.094)^2 + (Y_2 \times 0.094)^2}.$$

181 **Claim 3b:** A 95% CI for the true change in ADC of a prostate lesion is given below,
182 where Y_1 and Y_2 are the ADC measurements at the two time points:

183
$$(Y_2 - Y_1) \pm 1.96 \times \sqrt{(Y_1 \times 0.17)^2 + (Y_2 \times 0.17)^2}.$$

184 **Claim 4b:** A 95% CI for the true change in ADC of a breast lesion is given below,
185 where Y_1 and Y_2 are the ADC measurements at the two time points:

186
$$(Y_2 - Y_1) \pm 1.96 \times \sqrt{(Y_1 \times 0.048)^2 + (Y_2 \times 0.048)^2}.$$

187

188 **These claims hold when:**

- 189
- 190 • The same imaging methods on the same scanner and the same analysis methods are used at two
191 separate time points where the interval between measurements is intended to represent the evolution
192 of the tissue over the interval of interest (such as pre-therapy versus post initiation of therapy).
 - 193 • Conspicuity of lesion boundary is adequate to localize the lesion for definition on a region-of-
194 interest [27] at both time points.
 - 195 • For breast, a whole lesion/tissue (multi-slice) ROI is used [43, 44] at each timepoint.

196 **Discussion**

- 197
- 198 • These claims are based on estimates of the within-subject coefficient of variation (wCV) for ROIs
199 drawn in the brain, liver, prostate, and breast. For estimating the critical % change, the %
200 Repeatability Coefficient (%RC) is used: $2.77 \times \text{wCV} \times 100\%$, or %RC = 11% for brain, 26% for
201 liver, 47% for prostate, and 13% for breast. Specifically, it is assumed that the wCV is 4% for brain,
202 9.4% for liver, 17% for prostate, and 4.8% for the breast. The claim assumes that the wCV is
203 constant for tissue regions in the specified size, the signal-to-noise ratio (SNR) of the tissue region
204 on the $b=0$ image is at least 50, and that the measured ADC is linear (slope=1) with respect to the
205 true ADC value over the tissue-specific range $0.3 \times 10^{-3} \text{ mm}^2/\text{s}$ to $3.0 \times 10^{-3} \text{ mm}^2/\text{s}$.

- For the brain, estimates are from Bonekamp 2007, Pfefferbaum 2003 (mean ADC in an anatomical region or polygonal ROI), and Paldino 2009 [45-47]; for the liver, estimates are from Miquel 2012, Braithwaite 2009 (mean ADC in an ROI between 1-4 cm²) [48-51]; for the prostate, estimates are from Litjens 2012, Fedorov 2017 and Gibbs 2007 (Table 1 of the manuscript, mean ADC is from an ROI ranging from 120 to 320 mm², with little impact on repeatability) [52-56]. The claims of this Profile, informed by this cited literature, do not address heterogeneity in prostate; zone-specific ROIs may result in lower wCVs. For the breast, estimates are for mean ADC in a multi-slice ROI from Newitt 2018 [43] (covering the whole tumor) and Sorace 2018 [44] (normal breast fibroglandular tissue).
- In general, where there is test-retest data for ADC, there is usually not consistent accompanying information about ROI size and shape. It will be valuable to have such information to better inform future claim statements.

2.3 Clinical Interpretation

In tumors, changes in ADC can reflect variations in cellularity, as inferred by local tissue water mobility, e.g., a reduction or increase of the extracellular space, although the level of measured change must be interpreted relative to the Repeatability Coefficient before considered as a true change [1, 30, 34, 37, 43-48, 51, 56-58]. Other biological processes may also lead to changes in ADC, e.g., stroke.

Low ADC values suggest cellular dense tissue and potentially solid/viable tumor as opposed to elevated ADC values in tumor necrosis and cystic spaces. For example, ADC in the peripheral zone of the prostate decreases with the presence of cancer (while generally increasing with age) [59]. Care should be taken to correlate ADC findings with morphology, e.g., with T₂-weighted images in the prostate in the case of an abscess. The use of specific interpretation of ADC values will depend on the clinical application, e.g., taking into account spontaneous tumor necrosis versus tumor necrosis after effective therapy. Schema and properties of tissues to assay by ADC should be addressed during the design phase of each study. For example, therapies targeted to induce cytotoxic change in solid viable tumor [3, 19, 22, 38, 41] are candidate for ADC monitoring by ROI segmentation guided by traditional MR indicators of solid viable tissue, namely: relatively hyperintense on high *b*-value DWI, low ADC, and perfused on dynamic contrast-enhanced MRI. The anticipated timescale of *early* therapeutic response and/or tumor progression must be considered in study design of MRI scan dates for application of ADC as a prognostic marker.

238 **3. Profile Activities**

239 The Profile is documented in terms of “Actors” performing “Activities”. Equipment, software, staff or sites
 240 may claim conformance to this Profile as one or more of the “Actors” in the following table.

241 Conformant Actors shall support the listed Activities by conforming to all requirements in the referenced
 242 Section.

243 For some activity parameters, three specifications have been defined. Meeting the ACCEPTABLE
 244 specification is sufficient to conform to the profile. Meeting the TARGET or IDEAL specifications is
 245 expected to achieve improved performance, but are not required for conformance to the profile.

246 **ACCEPTABLE:** Actors that shall meet this specification to conform to this profile.

247 **TARGET:** Meeting this specification is achievable with reasonable effort and adequate equipment and is
 248 expected to provide better results than meeting the ACCEPTABLE specification.

249 **IDEAL:** Meeting this specification may require extra effort or non-standard hardware or software, but is
 250 expected to provide better results than meeting the TARGET.

251

252 **Table 1: Actors and Required Activities**

Actor (Checklist Appendix)	Activity	Section
Site (see F.1)	Qualification, Periodic QA	3.2, 3.5
Acquisition Device (see F.2)	Site Qualification	3.2
	Pre-delivery	3.3
	Periodic QA	3.5
	Protocol Design	3.6
	Image Data Acquisition	3.9
Scanner Operator* (see F.3)	Site Qualification	3.2
	Periodic QA	3.5
	Protocol Design	3.6
	Subject Selection and Handling	3.7 and 3.8
	Image Data Acquisition, Reconstruction, QA, and Distribution	3.9, 3.10, 3.11 and 3.12
	Staff and Site Qualification	3.1 and 3.2

Image Analyst [†] (see F.4)	Image QA, Distribution, and Analysis	3.11, 3.12, and 3.13
Reconstruction Software (see F.5)	Image Data Reconstruction	3.10
Image Analysis Tool (see F.6)	Image Analysis	3.13

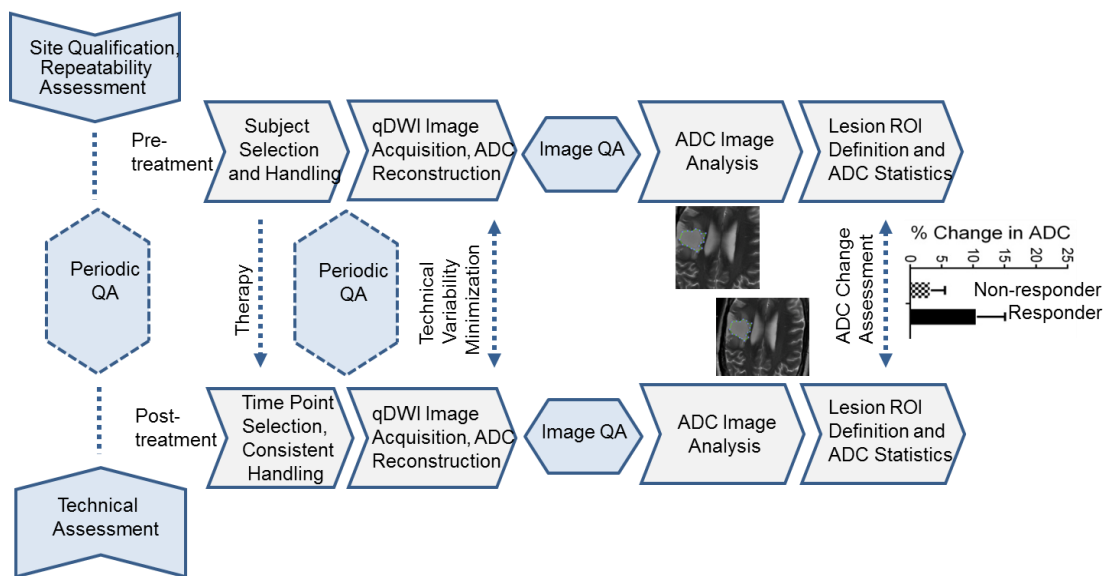
*Scanner operator may be an MR technologist, physicist, or other scientist

[†]Image analyst may be a radiologist, technologist, physicist, or other scientist.

253
254
255
256
257
258
259

The requirements in this Profile do not codify a Standard of Care; they only provide guidance intended to achieve the stated Claim. Failing to conform to a “shall” statement in this Profile is a protocol deviation. Handling protocol deviations for specific trials/studies is at full discretion of the study sponsors and other responsible parties.

260 Example of a clinical trial workflow based on this DWI Profile is shown in Figure 1:



261
262
263
264
265

Figure 1: Typical quantitative Diffusion-Weighted MRI trial workflow for Treatment Response Assessment with key QIBA profile activities

3.1. Staff Qualification

267 This activity involves evaluating the human Actors (Radiologist, Scanner Operator and Image Analyst)
268 prior to their participation in the Profile.

3.1.1 DISCUSSION

270 These requirements, as with any QIBA Profile requirements, are focused on DWI-relevant activities
271 required to achieve the DWI Profile Claims. Evaluating the medical or professional qualifications of
272 participating actors is beyond the scope of this profile.

273

274 In clinical practice, it is expected that the radiologist interpreting the examination often will be the image
 275 analyst. In some clinical practice situations, and in the clinical research setting, the image analyst may be a
 276 non-radiologist professional such as a medical physicist, biomedical engineer, MRI scientist or 3D lab
 277 technician. While there are currently no specific certification guidelines for image analysts, a non-
 278 radiologist performing diffusion analysis should be trained in technical aspects of DWI including:
 279 understanding key acquisition principles of diffusion weighting and directionality and diffusion test
 280 procedures (Appendix E); procedures to confirm that diffusion-related DICOM metadata content is
 281 maintained along the network chain from scanner to PACS and analysis workstation. The analyst must be
 282 expert in use of the image analysis software environment, including ADC map generation from DWI (if not
 283 generated on the scanner), and ADC map reduction to statistics with ROI/VOI location(s) retained. The
 284 analyst should undergo documented training by a radiologist having qualifications conforming to the
 285 requirements of this profile in terms of anatomical location and image contrast(s) used to select
 286 measurement target. The level of training should be appropriate for the setting and the purpose of the
 287 measurements. It may include instruction in topics such as directional and isotropic DWI and ADC map
 288 reconstruction and processing; normative ADC values for select tissues; and recognition of image artefacts.
 289 The Technologist is always assumed to be a Scanner Operator for subject scanning, while phantom scanning
 290 can be performed by Image Analyst.

291 **3.1.2 SPECIFICATION**

Parameter	Actor	Specification
Qualification	Image Analyst	Shall undergo documented training by a qualified radiologist in terms of anatomical location and image contrast(s) used to select measurement target; and by qualified physicist in understanding key DWI acquisition principles of diffusion weighting and directionality and diffusion test procedures, procedures to confirm that diffusion-related DICOM metadata content is maintained along the network chain from Scanner to PACS and analysis workstation and in use of the Image Analysis Tool, including ADC map generation from DWI (if not generated on the scanner), and ADC map reduction to statistics with ROI/VOI location(s)

292 **3.2. Site qualification**

293 This activity involves evaluating performance of the product Actors (Acquisition Device, Reconstruction
 294 Software, and Image Analysis Tool) by the Scanner Operator and Image Analyst initially at the site to
 295 ensure acceptance to the trial and baseline cross-site protocol standardization, but not directly associated
 296 with a specific clinical trial subject, that are necessary to reliably meet the Profile Claim.

297 **3.2.1 DISCUSSION**

298 Site qualification testing will be performed according to the trial-specific multi-site protocol prior to
 299 inclusion into trial to check site’s ability to implement standardized acquisition protocol and image analysis,
 300 as well as establish the baseline performance level. Steps toward multi-device standardization include
 301 meeting the baseline performance specifications for bias and repeatability using quantitative DWI phantom
 302 [60-62]. The listed specifications are based on the prior multi-system studies [61, 63-66]. The details on the
 303 platform-specific phantom scanning protocols and performance metrics assessment are provided in Section
 304 4 and Appendices D and E.

305 Key quantitative DWI performance metrics include: ADC bias at magnet isocenter, random error within
 306 ROI (precision), SNR at each *b*-value, ADC dependence on *b*-value and ADC spatial dependence. To
 307 conform to this Profile, system performance benchmarks for these metrics are provided in 3.2.2 to ensure

308 negligible contribution of technical errors to above defined confidence intervals measured for tissue. These
 309 benchmarks reflect the baseline MRI equipment performance in clinical and multi-center clinical trial
 310 settings to support the Claims of this Profile. To establish tighter confidence bounds for ADC metrics,
 311 additional technical assessment procedures may be introduced according to specific clinical trial protocol.
 312 Note that with other performance assessment metrics conformant to the Profile, the listed acceptable ranges
 313 for spatial ADC bias could be the major source of the technical measurement error limiting ADC confidence
 314 intervals in multi-center studies.

315 3.2.2 SPECIFICATION

Parameter	Actor	Requirement
Qualification activities	Site	Shall perform qualification activities for Acquisition Device, Scanner Operator, and Image Analyst to meet equipment, reconstruction SW, image analysis tool and phantom ADC performance metrics as specified in table 3.2.2 and by trial-specific protocol 3.6.2
DWI Tags	Acquisition Device	Shall preserve tags related to DWI, including private tags, which may be vendor-specific. Some key tags are specified in Appendix D.
Acquisition Protocols		Shall be capable of storing protocols and performing scans with all the parameters set as specified in section 3.6.2 "Protocol Design Specification" and Appendix D
Acquisition Device Performance	Scanner Operator	Shall prepare scan protocols conformant with section 3.6.2 "Protocol Design Specification" and phantom qualification (Appendix D) and ensure that DWI acquisition parameters (<i>b</i> -value, diffusion direction) shall be preserved in DICOM and shall be within ranges allowed by study protocol (both for phantom and subject scans).
Reconstruction SW Performance		Shall perform assessment procedures (Section 4) for site qualification and longitudinal QA for the acquisition devices participating in trial to document acceptable performance for phantom ADC metrics as specified in this table
Image Analysis Tool Performance	Image Analyst	Shall confirm that reconstruction SW is capable of performing reconstructions and producing images with all the parameters set as specified in section 3.6.2 "Protocol Design Specification" and meet DWI DICOM header and image registration requirements specified in 3.10.2, including storage of <i>b</i> -values, DWI directionality, image scaling and units tags, as specified in DICOM conformance statement for the given scanner SW version, as well as the model-specific Reconstruction Software parameters utilized to achieve conformance.
		Shall test Image Analysis Tool to ensure acceptable performance according to 3.13.2 specifications for study image visualization, DICOM and analysis meta-data interpretation and storage, ROI segmentation, and generation of ADC maps and repeatability statistics for qualification phantom (below)

Parameter	Actor	Requirement
Phantom ADC ROI		Shall confirm that phantom ROI is 1-2 cm diameter (>80 pixels without interpolation) for all specifications below
Phantom ADC metrics		Shall evaluate and record phantom ADC metrics (bias, linearity and precision) according to Table 3.2.2 specifications for Acquisition Device qualification and periodic QA using QIBA-provided or qualified site Image Analysis Tool
ADC bias at/near isocenter	Acquisition Device / Image Analyst	$ ADC\ bias \leq 0.04 \times 10^{-3} \text{ mm}^2/\text{s}$, or $\leq 3.6\%$ for ice-water phantom or other quantitative DWI phantom
ADC error at/near isocenter		ADC random error $\leq 2\%$ for ice-water phantom or other quantitative DWI phantom
Short-term (intra-exam) ADC repeatability at/near isocenter		$RC \leq 1.5 \times 10^{-5} \text{ mm}^2/\text{s}$ and $wCV \leq 0.5\%$ for ice-water phantom or other quantitative DWI phantom
Long-term (multi-day) ADC repeatability at/near isocenter		$RC \leq 6.5 \times 10^{-5} \text{ mm}^2/\text{s}$ and $wCV \leq 2.2\%$ for ice-water phantom or other quantitative DWI phantom
DWI $b=0$ SNR		$SNR (b=0) \geq 50 \pm 5$ for ice-water phantom or other quantitative DWI phantom.
ADC b -value dependence		$< 2\%$ for ice-water phantom or other quantitative DWI phantom over b -value pairs 0-500; 0-900; and 0-2000s/mm ²
Maximum bias with offset from isocenter: within 4 cm in any direction		$< 4\%$ for uniform DWI phantom
R/L offset < 10 cm (with A/P and S/I < 4 cm)		$< 10\%$ for uniform DWI phantom
A/P offset < 10 cm (with R/L and S/I < 4 cm)		$< 10\%$ for uniform DWI phantom
S/I offset < 5 cm (with R/L and A/P < 4 cm)		$< 10\%$ for uniform DWI phantom

316

317 **3.3. Pre-delivery**

318 Standard scanner calibrations, phantom imaging, performance assessments or validations prior to delivery
 319 of equipment to a site (e.g., performed at the factory) for routine clinical service are beyond the scope of
 320 this profile but are assumed to be satisfied.

321 **3.3.1 DISCUSSION**

322 Current clinical MR scanners equipped with single-shot echo planar DWI capabilities compliant with trial
 323 acquisition protocol are adequate to meet the Profile Claim.

324 **3.3.2 SPECIFICATION**

325

Parameter	Actor	Requirement
Performance metrics	Acquisition Device	Scanner shall meet established vendor performance metrics for given model
DWI sequence		Scanner shall be capable to acquire single-shot DWI
DICOM conformance		DICOM conformance statement from Vendor will include DICOM tags for <i>b</i> -value and diffusion direction(s).

326 **3.4. Installation**

327 Beyond standard installation activities which are outside the scope of this profile, network DICOM client
 328 configuration of PACS and analysis workstation(s) shall maintain all DWI-relevant DICOM metadata.

329 **3.5. Periodic QA**

330 This activity describes phantom imaging, performance assessments or validations performed after initial
 331 acceptance to the trial and periodically at the site, but not directly associated with a specific subject, that
 332 are necessary to reliably meet the Profile Claim.

333 **3.5.1 DISCUSSION**

334 Periodic quality assurance procedures should be consistent with those generally accepted for routine clinical
 335 imaging but are outside the scope of this profile. Additional DWI-specific QA procedures to ensure baseline
 336 scanner performance with minimal technical variability are described in Section 4 and Appendices D and
 337 E, and can be utilized as needed [21, 67]. Presently, there are insufficient data to require a set frequency of
 338 periodic QA, which is specific to the clinical trial design. However, QA procedures should be followed
 339 after a hardware or software upgrade.

340 **3.5.2 SPECIFICATION**

Parameter	Actor	Requirement
Periodic DWI QA	Site/Scanner Operator/ Acquisition Device	Shall perform system qualification and periodic QA that includes assessment of ADC bias, random error, linearity, DWI SNR, DWI image artefacts, <i>b</i> -value dependence and spatial uniformity (3.2.2)
Equipment	Site	Same, pre-qualified equipment and SW shall be used over the length of trial, and all preventive maintenance shall be documented over the course of the trial. Re-qualification shall be performed in case of major SW or hardware upgrade.

341 **3.6. Protocol Design**

342 This activity involves designing DWI acquisition and reconstruction procedures that are necessary to
343 reliably meet the Profile Claim. Along with site qualification (3.2), this activity facilitates cross-platform
344 protocol standardization for multi-site trials.

345 3.6.1 DISCUSSION

346 The Profile considers Protocol Design to take place at the imaging site, however, sites may choose to make
347 use of protocols developed elsewhere. DWI scan protocols (for phantom QA and subject scanning) should
348 be pre-built by the Scanner Operator during site qualification (3.2.2), clearly labeled and stored on the MRI
349 system for recall in study scans with minimal parameter changes within allowed specification ranges.
350 Version control of edits to the protocol should be tracked with prior versions archived. Standardized DWI
351 phantom scan protocols are tabulated in Appendix D.

352
353 Tables in section 3.6.2 contain key specifications for subject DWI scan protocols expressed using generic
354 terminology. The specifications are consistent with publications supporting Profile Claims and consensus
355 recommendations for brain [31, 45-47, 68], liver [21, 28, 48-51, 58] and prostate [52-56, 59]. Some
356 parameters include a numerical range. Reduction of respiratory artefact in the liver requires either short
357 breath-hold (un-averaged, <25 sec), or long (3-5 min) respiratory-synchronization, or free breathing with
358 high signal averaging. The gain in image quality with high signal averaging favors use of non-breath-hold
359 abdominal DWI. New techniques, such as simultaneous multi-slice or multi-band MRI, are becoming
360 commercially available and could be advantageous for DWI [69-72]. *k*-space undersampling, rFOV, and
361 multi-shot EPI techniques are also becoming more common [73-79]. However, these are not yet considered
362 “standard” on most clinical systems and therefore are not specified below. The literature which informs the
363 prostate claim in Section 2 presents 3T data with body coil exclusively; therefore, the associated prostate
364 protocols in this Profile are limited to 3T. This Profile does not yet address the use of DWI at high (>3 T)
365 or low-field (<1.5 T) strengths due to the absence of test-retest literature.

366
367 Care should be taken to utilize the same scan parameters across exams, particularly within a study. For
368 example, close attention should be paid to the TE, which should be consistent across exams.

369
370 In the specification tables, there are requirements to include $b=0$ s/mm² images. This hastens image
371 acquisition by obviating acquisition of multiple directions to enable directional averaging of non-zero *b*-
372 values, however low. However, some scanners do not produce a “true-zero” *b*-value. Whenever possible,
373 true-zero *b*-value should be acquired; when hardware or software makes this not possible, $b<50$ s/mm² can
374 be acquired in lieu of true-zero *b*-values.

375
376 In the case of breast imaging (3.6.2.4), phase encoding along the anterior-posterior axis preserves anatomic
377 symmetry for axial breast fields of view, and is preferred over left-right phase encoding (which is still
378 acceptable).

379 3.6.2 SPECIFICATION

ACCEPTABLE: Actors that shall meet this specification to conform to this profile.

TARGET: Meeting this specification is achievable with reasonable effort and adequate equipment and is expected to provide better results than meeting the ACCEPTABLE specification.

IDEAL: Meeting this specification may require extra effort or non-standard hardware or software, but is expected to provide better results than meeting the TARGET.

381
382

3.6.2.1 Brain

Parameter	Actor	Requirement	DICOM Tag [†]
Field Strength	Acquisition Device/Scanner Operator	1.5 or 3T	[0018, 0087]
Acquisition sequence		Diffusion-weighted Single-Shot Echo Planar Imaging (SS-EPI)	[0018, 0020]
Receive Coil type		Ideal: 32 channel head array coil	[0018, 1250]
		Target: 8-32 channel head array coil	
		Acceptable: 8 channel head array coil	
Lipid suppression		On	
Number of <i>b</i> -values		Ideal: ≥ 3 (including one $b=0-50$; one 450-550 s/mm ² ; and one at highest <i>b</i> -value)	
		Acceptable/Target: 2 (including $b=0-50$ s/mm ² and at highest <i>b</i> -value)	
Minimum highest <i>b</i> -value		Target/Ideal: $b=1000$ s/mm ²	[0018, 9087]
		Acceptable: $b=850-999$ s/mm ²	
Diffusion directions		Target/Ideal: ≥ 3 -orthogonal, combined gradient channels	[0018, 9075]
		Acceptable: ≥ 3 -orthogonal, single gradient channels	[0018, 9089]
Slice thickness		Ideal: ≤ 4 mm	[0018, 0050]
		Target: 4-5 mm	
		Acceptable: 5mm	
Gap thickness		Target/Ideal: 0-1 mm	[0018, 0088]
		Acceptable: 1-2 mm	
Field-of-view		Ideal/Target/Acceptable: 220-240 mm FOV along both axes	[0018, 1100]
Acquisition matrix		Target/Ideal: (160-256) x (160-256), or 1.5-1 mm in-plane resolution	[0018, 1310]
		Acceptable: 128 x 128, or 1.7 mm in-plane resolution	
Plane orientation	Transversal-axial	[0020, 0037]	
Phase-encode/ frequency-encode direction	Anterior-Posterior / Right-Left	[0018, 1312]	
Number of averages	Ideal/Target: ≥ 2	[0018, 0083]	
	Acceptable: 1		

Half-scan factor		Acceptable/Target: >0.65	[0018, 9081]
In-plane parallel imaging acceleration factor		Ideal: 2-3 Acceptable/Target: 2	[0018, 9069]
TR		Ideal: > 5000 ms Acceptable/Target: 3000-5000 ms	[0018, 0080]
TE		Ideal: <60ms	[0018, 0081]
		Target: minimum TE	
Receiver Bandwidth		Ideal/Target: maximum possible in frequency encoding direction (minimum echo spacing)	[0018, 0095]
		Acceptable:>1000 Hz/voxel	

383

384

385

3.6.2.2 Liver

Parameter	Actor	Requirement	DICOM Tag ⁺
Field Strength	Acquisition Device/Scanner Operator	1.5 or 3 T	[0018, 0087]
Acquisition sequence		Diffusion-weighted Single-Shot Echo Planar Imaging (SS-EPI)	[0018, 0020]
Receive Coil type		Ideal: >16 channel torso array coil Target: 6-16 channel torso array coil Acceptable: 6 channel torso array coil	[0018, 1250]
Lipid suppression		On	
Number of <i>b</i> -values		Ideal: ≥ 3 (including one $b=0-50$; one 100-300 s/mm^2 ; and one at highest b -value)	[0018, 9087]
		Acceptable/Target: 2 (including one $b=50-100s/mm^2$ and one at highest b -value)	
Minimum highest <i>b</i> -value		Target/Ideal: $b=600-800 s/mm^2$	[0018, 9087]
		Acceptable: 500 s/mm^2	
Diffusion directions		Target/Ideal: 3-orthogonal, combined gradient channels	[0018, 9075]
		Acceptable: 3-orthogonal, single gradient channels	[0018, 9089]
Slice thickness	Ideal: <5 mm	[0018, 0050]	
	Target: 5-7 mm		
Gap thickness	Acceptable: 7-9 mm	[0018, 0088]	
	Ideal: 0 mm		
	Target: 1 mm		
		Acceptable:>1-2 mm	

Field-of-view		Ideal/Target/Acceptable: 300-450 mm	[0018, 1100]
Acquisition matrix		Target/Ideal: (160-196) x (160-192), or 2.5-2 mm in-plane Acceptable: 128 x 128, or 3-2.6 mm in-plane resolution	[0018, 1310]
Plane orientation		Transversal-axial	[0020, 0037]
Half-scan factor		Acceptable/Target: >0.65	[0018, 9081]
Phase-encode/ frequency-encode direction		Anterior-Posterior / Right-Left	[0018, 1312]
Number of averages		Ideal: > 4	[0018, 0083]
		Target: 4	
		Acceptable: 2-3	
Parallel imaging factor		Ideal: 2-3	[0018, 9069]
		Target/Acceptable: 2	
TR		Ideal/Target/Acceptable > 2000 ms	[0018, 0080]
TE		Ideal: < 60 ms	[0018, 0081]
		Target: minimum TE	
		Acceptable: < 110 ms at 1.5 T; <90 ms at 3 T	
Receiver Bandwidth		Ideal/Target: maximum possible in frequency encoding direction (minimum echo spacing)	[0018, 0095]
		Acceptable: > 1000 Hz/voxel	

386

387

388

3.6.2.3 Prostate

Parameter	Actor	Requirement [‡]	DICOM Tag ⁺
Field Strength		3 T	[0018, 0087]
Acquisition sequence		Diffusion-weighted Single-Shot Echo Planar Imaging (SS-EPI)	[0018,0020]
Receive Coil type		Ideal/Target: ≥8 channel torso array coil Acceptable: <8 channel pelvic phased array coil/endorectal coil; body array coil	[0018,1250]
Lipid suppression		On	
Number of <i>b</i> -values [‡]	Acquisition Device/Scanner Operator	Ideal: ≥3 (including one <i>b</i> =0-50; one 100-500 s/mm ² ; and one at highest <i>b</i> -value)	
		Acceptable/Target: 2 (including one <i>b</i> <50-100s/mm ² and one at highest <i>b</i> -value)	
Minimum highest <i>b</i> -value [‡]		Ideal: <i>b</i> =1000-1500 s/mm ²	[0018, 9087]
		Target/Acceptable: 500-1000 s/mm ²	

Diffusion directions	Target/Ideal: 3-orthogonal, combined gradient channels Acceptable: 3-orthogonal, single gradient channels	[0018, 9075] [0018, 9089]
Slice thickness [‡]	Ideal: ≤3 mm	[0018, 0050]
	Target: 3-4 mm	
	Acceptable: 4-5 mm	
Gap thickness	Ideal: 0 mm	[0018, 0088]
	Target/Acceptable: 1 mm	
Field-of-view [‡]	Ideal/Target/Acceptable: 240-260 mm	[0018, 1100]
Acquisition matrix [‡]	Target/Ideal/Acceptable: (224-128) x (224-128), or 2-1 mm in-plane	[0018, 1310]
Plane orientation	Transversal-axial	[0020, 0037]
Half-scan factor	Acceptable/Target: >0.65	[0018, 9081]
Phase-encode/ frequency-encode direction	Anterior-Posterior / Right-Left	[0018, 1312]
Number of averages	Ideal: > 4	[0018, 0083]
	Target: 4	
	Acceptable: 2-4	
Parallel imaging factor	Ideal /Target/Acceptable: 2	[0018, 9069]
TR [‡]	Ideal/Target/Acceptable > 2000 ms	[0018, 0080]
TE	Ideal: < 60 ms	[0018, 0081]
	Target: minimum TE	
	Acceptable: ≤ 90 ms	
Receiver Bandwidth	Ideal/Target: maximum possible in frequency encoding direction (minimum echo spacing)	[0018, 0095]
	Acceptable: > 1000 Hz/voxel	

389
390
391
392
393
394
395
396

[†]Only public DICOM tags are listed above. Vendors storing key acquisition meta-data in non-standard (private tags) should provide DICOM conformance statement listing the corresponding header items.

[‡]PI-RADS recommendations can differ from the protocols derived from the cited literature in this Profile. The PI-RADS v2 recommendations can be found at:

<https://www.acr.org/~media/ACR/Documents/PDF/QualitySafety/Resources/PIRADS/PIRADS%20V2.pdf>

397
398

3.6.2.4 Breast

Parameter	Actor	Requirement	DICOM Tag [†]
Field Strength	Acquisition Device/Scanner Operator	1.5 or 3 T	[0018, 0087]
Acquisition sequence		Diffusion-weighted Single-Shot Echo Planar Imaging (SS-EPI)	[0018, 0020]
Receive Coil type		Ideal/Target: 5-16 channel bilateral breast coil Acceptable: 4 channel bilateral breast coil	[0018, 1250]
Lipid suppression		Ideal/Target: combined spectral and relaxation-based fat suppression (e.g., SPAIR) Acceptable: Relaxation-based (STIR) or spectral-based (fat-sat) alone if SPAIR is not available	
Number of <i>b</i> -values		Ideal: ≥ 4 Target/Acceptable: ≥ 3 (including one $b=0-50$; one 100 s/mm^2 ; and one at highest b -value)	
		Acceptable: 2 (including one $b=0-50 \text{ s/mm}^2$ and one at highest b -value)	
Minimum highest <i>b</i> -value		Target/Ideal: $b=600-800 \text{ s/mm}^2$	[0018, 9087]
		Acceptable: 600 s/mm^2	
Diffusion directions		Target/Ideal: 3-orthogonal, combined gradient channels Acceptable: 3-orthogonal, single gradient channels	[0018, 9075] [0018, 9089]
		Ideal: 4 mm Target: 4-5 mm Acceptable: 5 mm	[0018, 0050]
Slice thickness		Ideal: 0 mm Target: 0-1 mm Acceptable: 1 mm	[0018, 0088]
		Ideal/Target/Acceptable: 260-360 mm *complete bilateral coverage	[0018, 1100]
Acquisition matrix		Target/Ideal: (128-192) x (128-192), or 2.8-1.8 mm in-plane Acceptable: 128 x 128, or 2.8 mm in-plane resolution	[0018, 1310]
Plane orientation		Transversal-axial	[0020, 0037]
Half-scan factor		Acceptable/Target: >0.65	[0018, 9081]

Phase-encode/ frequency-encode direction		Ideal/Target: Anterior-Posterior/Right-Left Acceptable: Right-Left /Anterior-Posterior	[0018, 1312]
Number of averages		Ideal/Target: 3-5	
		Acceptable:2	[0018, 0083]
Parallel imaging factor		Ideal: ≥ 2	[0018, 9069]
		Target/Acceptable: 1.5-2	
TR		Ideal/Target/Acceptable ≥ 4000 ms	[0018, 0080]
TE		Ideal/Target: minimum TE (50-100ms)	
		Acceptable: < 114 ms	[0018, 0081]
Receiver Bandwidth		Ideal/Target: maximum possible in frequency encoding direction (minimum echo spacing)	[0018, 0095]
		Acceptable: > 1000 Hz/voxel	

399 **3.7. Subject Selection**

400 This activity describes criteria and procedures related to the selection of appropriate imaging subjects.
401 General MRI subject safety is assumed to be observed, but is beyond the scope of this DWI-specific Profile.

402 3.7.1 DISCUSSION

403 Despite having an acceptable risk status, metal-containing implants and devices near the tissue/organ/lesion
404 of interest may introduce artefact and may not be suitable for DWI.

405 For specific study/trial, subject scan timing should be appropriately synchronized with the assayed subject
406 condition (e.g., clinical state or therapeutic phase) per study design.

407 **3.8. Subject Handling**

408 This activity describes details of handling imaging subjects that are necessary to meet this Profile Claims.
409 General MRI subject safety considerations apply but are beyond the scope of this Profile.

410 3.8.1 DISCUSSION

411 Brain, liver, and breast DWI do not require special subject handling. To reduce motion artefact from bowel
412 peristalsis during prostate imaging, the use of an antispasmodic agent may be beneficial in some patients.
413 The presence of air and/or stool in the rectum may induce artefactual distortion that can compromise DWI
414 quality. Thus, some type of minimal preparation enema administered by the patient in the hours prior to the
415 exam maybe beneficial. However, an enema may also promote peristalsis, resulting in increased motion
416 related artefacts in some instances. The patient should evacuate the rectum, if possible, just prior to the MRI
417 exam.

418 **3.9. Image Data Acquisition**

419 This activity describes details of the subject/patient-specific image acquisition process that are necessary to
420 reliably meet the DWI Profile Claim.

421 3.9.1 DISCUSSION

422 Starting from the pre-built scan protocol, the technologist (scanner operator) will orient and position
 423 receiver coil study subjects uniformly. Patient-size parameter adjustments will be within allowed parameter
 424 ranges, and the same adjustments will be used for serial scans of given subject. To reduce spatial bias, when
 425 possible, the landmark will be placed close to the center of the target organ (e.g., prostate).

426 3.9.2 SPECIFICATION

Parameter	Actor	Requirement
Scan Procedure	Acquisition Device	Study of individual patient shall be performed on the site pre-qualified scanner using the approved receiver coil and pre-built profile-conformant scan protocol (3.6.2).
Patient Positioning	Scanner Operator (Technologist)	Predefined positioning procedure and receiver coil (e.g., always head-first or always feet-first, torso phased-array) shall be used for all study subjects. Subject-specific landmark shall be centered on the target organ, which shall be located as close as is feasible to magnet isocenter.
Scan Parameters		Subject-specific adjustments within allowed parameter ranges (Table 3.6.2) shall be made to suit body habitus. Parameter adjustments for a given subject shall be constant for serial scans.†
Acquisition Device		The same scanner shall be used for baseline measurement and a subsequent longitudinal measurement for detecting change in ADC.†

427 † Not using the same scanner and image acquisition parameters for baseline and subsequent measurements
 428 does not preclude clinical use of the measurement but will exclude meeting the requirements of the Profile
 429 claim.
 430

431 **3.10. Image Data Reconstruction**

432 This activity describes criteria and procedures related to producing images from the acquired data that are
 433 necessary to reliably meet the DWI Profile Claims.

434 3.10.1 DISCUSSION

435 At a minimum, three-orthogonal directional DWI are acquired and reconstructed individually for each
 436 imaged slice, then combined into a directionally-independent (i.e. isotropic or trace) DWI [80, 81].
 437 Diffusion weighted images may be interpolated to an image matrix greater than the acquired matrix.
 438 Directionally-independent trace or isotropic DWI are often automatically generated and retained by
 439 reconstruction software on the scanner for each non-zero *b*-value, whereas retention of directional DWI is
 440 optional. ADC maps are typically generated on the scanner using a mono-exponential model trace DWI vs.
 441 *b*-value. Alternatively, full DWI sets (directional plus trace, or trace alone) at all *b*-values can be provided
 442 for off-line ADC map generation (via mono-exponential model) on an independent workstation or thin-
 443 client distributed application.

444 Eddy currents and/or subject motion may create spatial misalignment or distortion between the individual
 445 directional DWI, and across *b*-values [82-84]. Direct combination of misaligned directional DWI will lead
 446 to spatial blur in trace DWI and subsequent artefact in ADC maps [82-84]. Spatial registration of directional
 447 DWI and/or trace DWI across all *b*-values may be performed on the scanner or off-line to reduce blur and
 448 improve quality of trace DWI and ADC maps.

449 Perfusion is known to affect diffusion measurement (a positive bias) particularly in highly vascular tissues
 450 (e.g., kidney and liver) [85-90]. ADC values derived from DWI spanning low b -value (i.e. $b < 50 \text{ s/mm}^2$) and
 451 modest high b -value (i.e. $b < 500 \text{ s/mm}^2$) increase perfusion bias. For diffusion measurement in liver, ADC
 452 maps should be reconstructed from DWI spanning $50\text{-}100 \text{ s/mm}^2$ up to $800\text{-}900 \text{ s/mm}^2$ to mitigate perfusion
 453 bias while maintaining adequate sensitivity to diffusion contrast and SNR. The degree of potential perfusion
 454 contamination of ADC will depend on blood volume fraction, number and distribution of b -values.
 455 Perfusion bias in brain DWI is considered small and typically ignored. There is a small deviation from
 456 mono-exponential decay (pseudo-diffusion) at low b -values in prostate [91].

457 3.10.2 SPECIFICATION

Parameter	Actor	Requirement
Trace DWI and ADC map generation across subjects and time	Scanner Operator	Procedural steps for image reconstruction, archiving of original, uncorrected images (if generated), and ADC map generation shall be held constant for all subjects and time points including: image interpolation; image registration prior to combination into trace DWI and across b -values; selection of b -values and fit algorithm to estimate ADC. ADC shall be calculated using the mono-exponential model of DWI signal decay with increasing b -value, starting with protocol-specific low b -value to compensate for perfusion effects.
b -value record		Scanner operator shall verify that the reconstruction SW records b -values, or if not shall manually record the b -values, that are used to generate the ADC map.
Trace DWI	Reconstruction Software	Trace DWI shall be automatically generated on the scanner and retained for each non-zero b -value. For equal b -value on three orthogonal DWI directions, the trace DWI is the geometric average of 3-orthogonal directional DWI at same b -value.
DICOM DWI		Exported DWI DICOM content shall provide acquired b -values and directionality.
Spatial Registration		Spatial misalignment between directional DWI and across b -values due to eddy currents or patient motion shall be corrected by image registration prior to generation of trace DWI and ADC maps.

458 **3.11. Image QA**

459 This activity describes criteria and evaluations of the images necessary to reliably meet the Profile Claim.

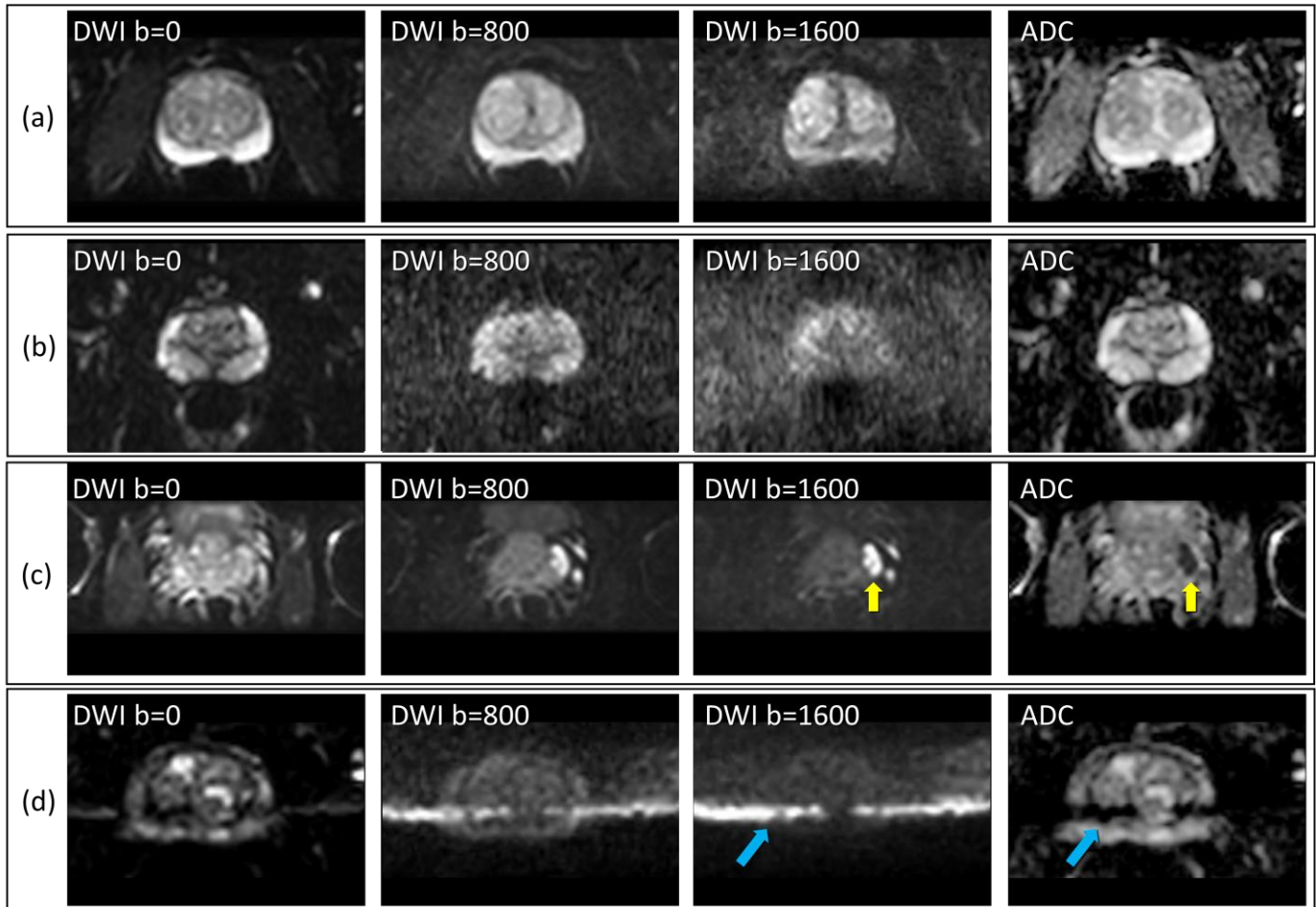
460 3.11.1 DISCUSSION

461 At the time of image acquisition and review, quality of DWI data should be checked for the following
 462 issues. Poor quality due to sources below may be grounds to reject individual datasets:

- 463 • Low SNR – Diffusion weighting inherently reduces signal, although signal must remain adequately
 464 above the noise floor to properly estimate ADC [92-94]. In general, the SNR at $b=0 \text{ s/mm}^2$ should
 465 be greater than 50. Low SNR (<5) at high b -values can bias ADC estimates. Visualization of
 466 anatomical features in tissues of interest at all b -values is acceptable evidence that SNR is adequate
 467 for ADC measurement (Figure 2 and Figure 3). Appendix E.2 provides instructions for measuring
 468 SNR in diffusion-weighted imaging, as well as guidance for the use of an appropriate DRO.

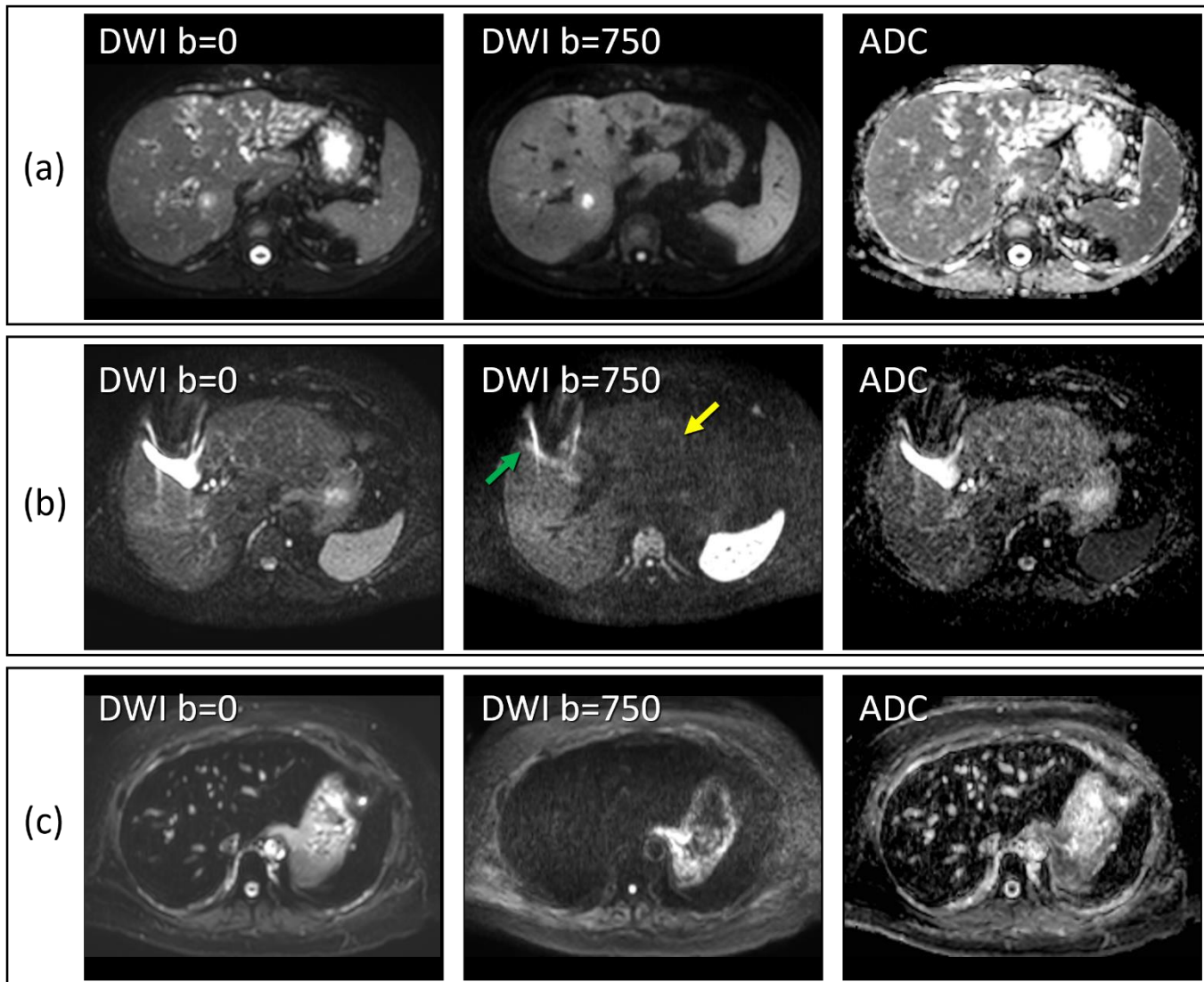
- 469
- 470
- 471
- Ghost/parallel imaging artefacts – Discrete ghosts from extraneous signal sources along phase-encode direction can obscure tissue of interest leading to unpredictable ADC values [83, 95-100] (Figure 2d, Figure 4, and Figure 8a).
- 472
- 473
- 474
- 475
- 476
- Severe spatial distortion – Some level of spatial distortion is inherent to SS-EPI, although distortion can be severe near high susceptibility gradients in tissues or metallic objects (Figure 3b, Figure 8c); or due to poor magnet homogeneity [83, 97]. Severe distortion can alter apparent size/shape/volume of tissues of interest thereby confound ROI definition, as well as adversely affect ADC values. Co-registration to high-resolution (non-EPI) T2-weighted image volume may reduce these distortions.
- 477
- 478
- 479
- 480
- 481
- 482
- 483
- Eddy currents – Distinct eddy currents amplified by strong diffusion pulses on different gradient channels lead to spatial misalignment across acquired DWI directions and b -values, and are manifest as spatial blur on trace DWI and erroneous ADC values particularly at the edges of anatomical features [83, 101] (Figure 5, Figure 9). Distortion correction and image registration to $b=0$ image prior to calculation of trace DWI and ADC maps may reduce these errors. Further artefact mitigation may be achieved by the use of double-spin echo bipolar-gradient pulse sequences, in particular at high b -values.
- 484
- 485
- 486
- 487
- 488
- 489
- 490
- 491
- Fat suppression – Lipid exhibits extremely low diffusion, with fat spatially shifted on SS-EPI from its true source (by several cm along the phase-encode direction) due to chemical shift [102-106]. Of note, scanner frequency drifting due to the heating from high duty cycle diffusion gradients could cause unsatisfactory fat suppression in the later frames of a diffusion acquisition, if only chemical shift saturation technique is used for fat suppression. In such case, alternative or additional fat suppression techniques, e.g., gradient reversal, could help to mitigate residual fat signal. Superposition of unsuppressed fat signal onto tissue of interest (Figure 6, Figure 8b) can invalidate ADC assessment there by partial volume averaging.
- 492
- 493
- 494
- 495
- 496
- 497
- 498
- 499
- 500
- 501
- 502
- 503
- Motion artefacts — While SS-EPI is effective at freezing most bulk motion, variability of motion over DWI directions and b -values contribute to blur and erroneous signal attenuation. Motion artefact is anticipated to be low in brain DWI for most subjects, although cardiac-induced pulsation can confound ADC measurement in/near ventricles and large vessels and in the brainstem. Respiratory and cardiac motion artefacts are more problematic in the liver, particularly the left-lobe and superior right lobe [12, 28, 97, 107, 108]. Quiet steady breathing or respiratory synchronization and additional signal averaging are used to mitigate motion artefact in abdominal DWI. Residual motion artefact can be recognized as inconsistent location of anatomical targets across b -values and DWI directions and/or spatial modulation unrelated to anatomical features on DWI/ADC maps. Inspection of DWI/ADC on orthogonal multi-planar reformat images aids detection of this artefact (Figure 7). Anti-peristaltic drugs and voiding of the rectum reduce motion- and susceptibility-induced artefacts when imaging the prostate, respectively.
- 504
- 505
- 506
- 507
- 508
- Nyquist ghost – EPI sequences acquire data using alternating readout gradient polarity between odd and even k -space lines. The associated eddy currents and resultant magnetic fields produce inconsistent phase shifts between even and odd echoes resulting in ghost artefacts that are referred to as Nyquist or $N/2$ ghosts (Figure 8a). Use of parallel imaging techniques results in additional copies of the $N/2$ ghost [100, 109].

510 Examples of common artefacts that may affect ADC maps are provided below:



511

512 Figure 2: Visual assessment of SNR in prostate DWI; (a) an example of good SNR at all b -values; (b) poor
 513 SNR at $b=1600 \text{ s/mm}^2$ where anatomical features of gland are barely above noise floor thus are prone to
 514 biased ADC values; (c) modest SNR in normal gland at $b=1600 \text{ s/mm}^2$ although good SNR in lesion due
 515 to low ADC (yellow arrows); (d) poor SNR at $b=1600 \text{ s/mm}^2$ plus a ghost artefact (blue arrows) leads to
 516 bias and artefactual ADC.



517

518 Figure 3: Visual assessment of SNR in liver DWI; (a) an example of good SNR at low and high b -values;
 519 (b) poor SNR particularly in left lobe at $b=750$ s/mm² (yellow arrow) and distortion due to metal (green
 520 arrow); and (c) poor SNR at both b -values where anatomical feature of the liver are lost.

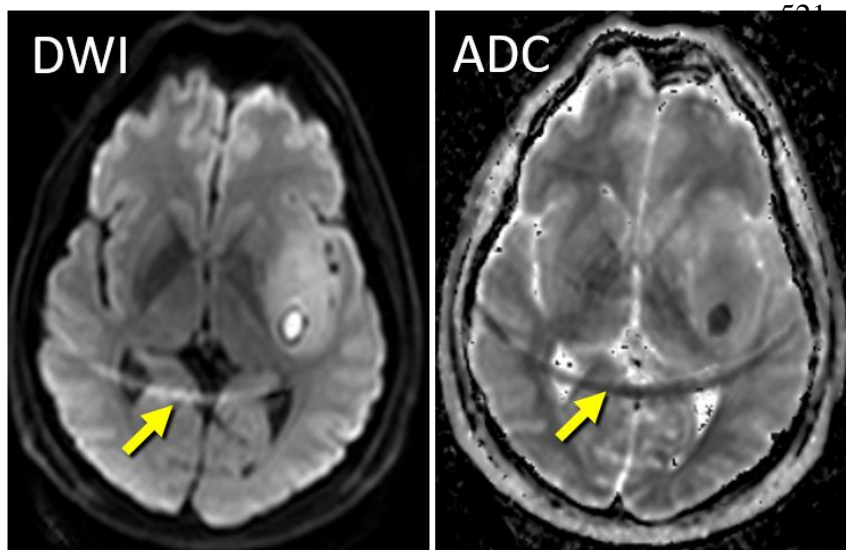
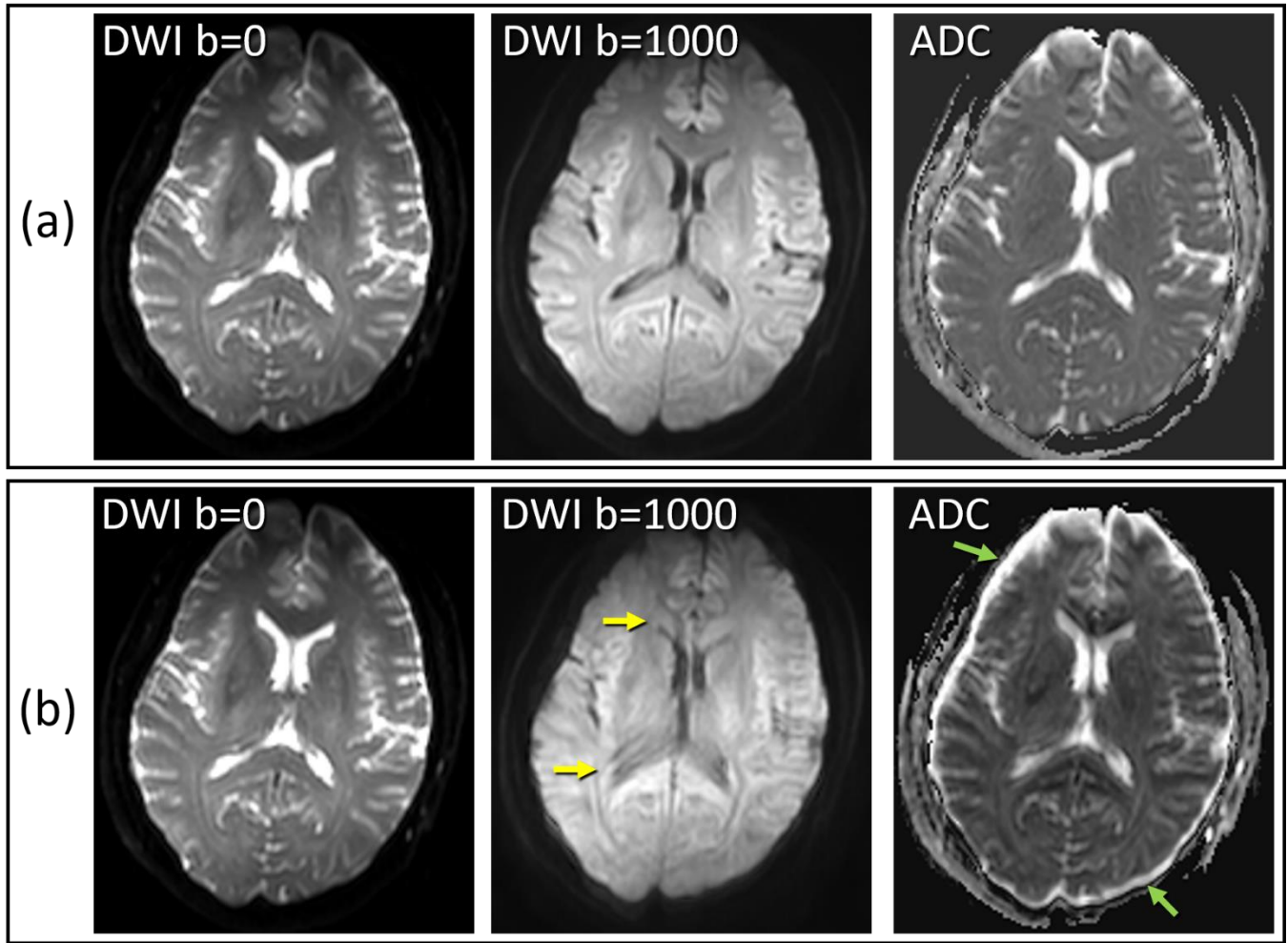
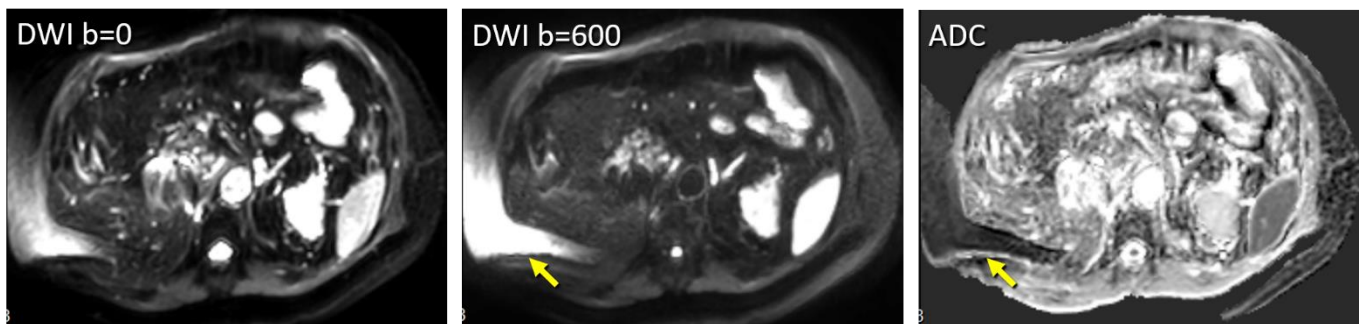


Figure 4: Ghost/parallel imaging artefact (arrows) replicates and shifts distant anatomical structures (posterior scalp in this example) along the phase-encode direction, thereby creating erroneous ADC values



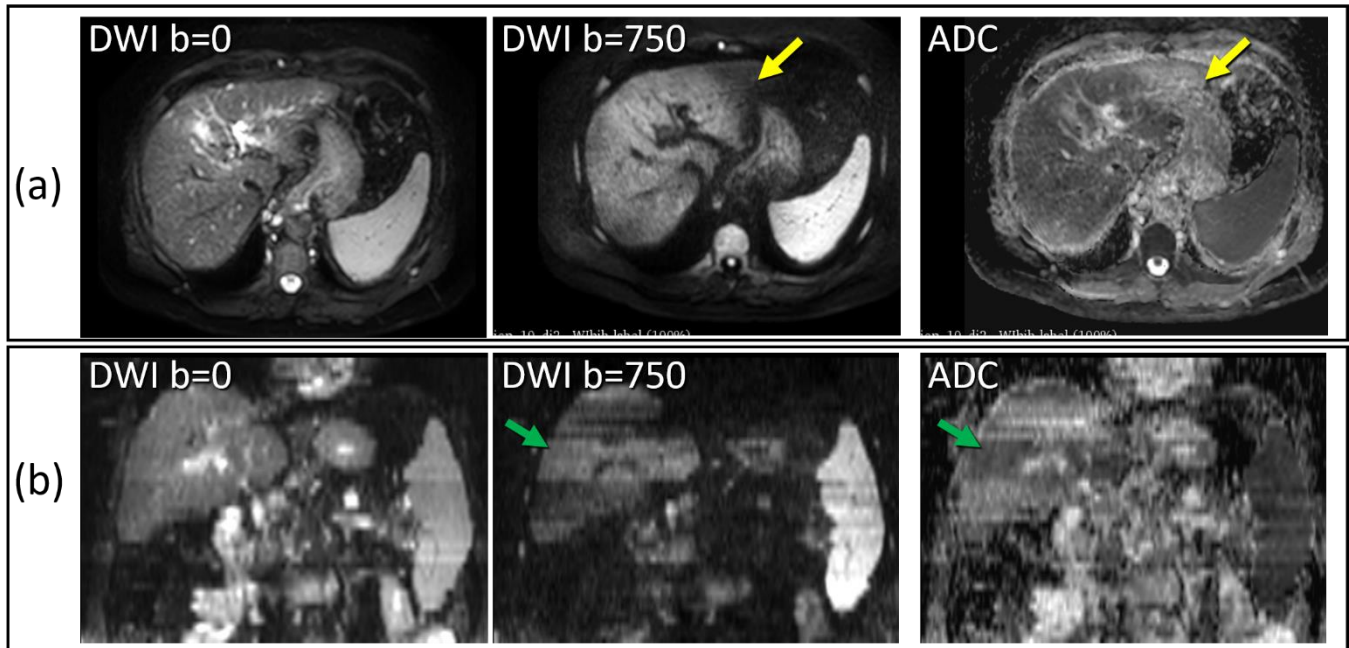
529

530 Figure 5: visual evidence of eddy currents in brain DWI. (a) Good quality DWI with no evidence of blur or
 531 spatial misalignment between low and high b -value DWI, thus no or low eddy current artefact. (b) Blur of
 532 anatomy on high b -value DWI (yellow arrows) relative to the $b=0$ DWI, plus blur and exaggerated thickness
 533 of the CSF rind around the brain (green arrows) relative to the CSF space on $b=0$ DWI are evidence of an
 534 eddy current artefact.



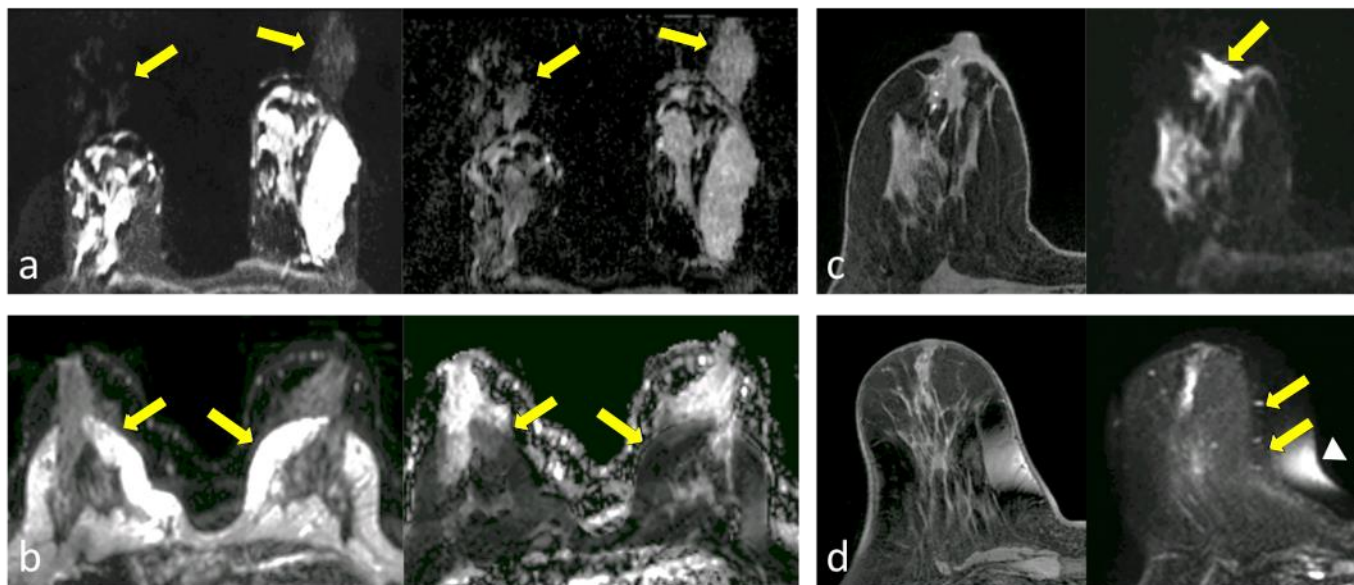
535

536 Figure 6: Unsuppressed fat signal spatially shifted on SS-EPI DWI (shifts several cm along phase-encode
 537 direction) can obscure the tissue of interest (arrow). Exceptionally low ADC of fat renders ADC
 538 meaningless in tissue superimposed by a residual fat signal.



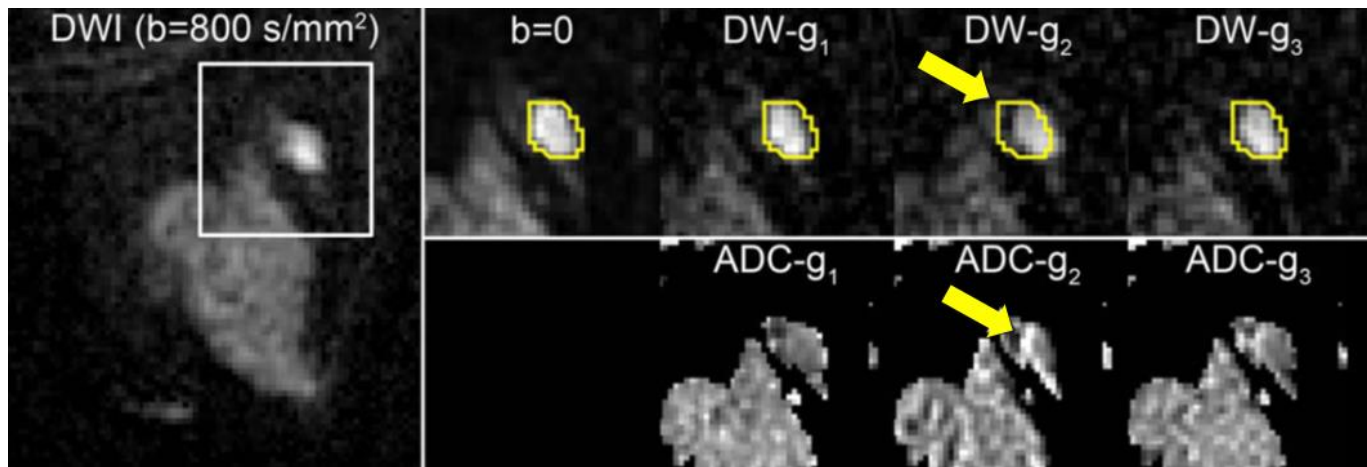
539

540 Figure 7: Visual assessment of motion artefact in liver DWI. (a) Areas of low signal on high b -value relative to adjacent tissue may result from motion. Cardiac pulsation transmitted to left lobe artefactually inflates
 541 ADC (yellow arrows).
 542
 543 (b) Reformat of axial DWI/ADC to coronal can aid identification of motion artefact seen as bands on high b -value and ADC (green arrows).



544

545 FIGURE 8: Common artefacts of breast DWI, illustrated in separate subjects. (a) Nyquist ghost artefact,
 546 appearing at N/4 due to parallel imaging undersampling, duplicating signal from the parenchyma on DWI
 547 (left) and resulting ADC map (right). (b) Detrimental chemical shift artefacts on DWI (left, arrows) due to
 548 poor fat suppression, causing artefactual reductions of ADC within the breast parenchyma (right, arrows).
 549 (c) Magnetic susceptibility artefact (arrow) causing distortion at air/tissue skin surface on DWI (right)
 550 compared with undistorted T1-weighted image (left). (d) Spatial distortion (arrows) and chemical shift
 551 artefact (arrowhead) of DWI due to poor shimming compared with undistorted T1-weighted image (left).
 552 (Figure adapted from Partridge et al. J. MAGN. RESON. IMAGING 2017;45:337–355 [110])
 553



554
555

556 FIGURE 9: Spatial misregistration between images within a DWI sequence representing eddy-current
 557 artefact. A breast lesion is visible in the lateral breast on the averaged DW image ($b=800 \text{ s/mm}^2$, left). White
 558 box shows region of magnification. A contour of the lesion defined on $b=0$ and propagated to the individual
 559 gradient direction DW images for the same slice shows the lesion is shifted (arrow) in the DW- g_2 image
 560 (obtained with diffusion gradients applied in the g_2 direction) with respect to the $b=50 \text{ s/mm}^2$ image and
 561 other $b=800 \text{ s/mm}^2$ images (obtained with gradients in the orthogonal g_1 and g_3 directions), owing to eddy-
 562 current effects. This misalignment causes an artefactual increase in ADC at the edge of the lesion on the
 563 corresponding ADC map (below). (Figure adapted from Partridge et al., J. Magn Reson Imaging
 564 2017;**45**:337–355 [110])
 565

566 **3.11.2 SPECIFICATION**

567

Parameter	Actor	Requirement
ADC quality	Image Analyst and/or Scanner Operator	Shall confirm DWI and ADC maps conform to adequate quality specifically considering points listed above (3.11.1) and shall exclude artefact-rich images and ROI from repeatability analysis.

568

569 **3.12. Image Distribution**

570 This activity describes criteria and procedures related to distributing, transferring and archiving images and
 571 metadata that are necessary to reliably meet the Profile Claim.

572 **3.12.1 DISCUSSION**

573 Images are distributed via network using the Digital Imaging and Communications in Medicine (DICOM)
 574 transfer protocol as per standard local practice. Along with required trace DWI DICOM, individual
 575 directional DWI and ADC maps (if generated on the scanner as DICOM images) should be archived. DWI
 576 DICOM tags that store this information currently vary among vendors. Directional DWIs may inform users
 577 about motion, eddy currents, or gradient non-linearities that are specific to a given direction, particularly
 578 when assessing scanner performance by use of a phantom with known properties.

579 Absolute image scaling and units of generated ADC maps must be available and ideally stored in public
 580 DICOM tags such as RealWorldValueMapping [0040,9096], RescaleIntercept [0028,1052], RescaleSlope

581 [0028,1053] and RescaleType [0028,1054] such that ADC map values are properly interpretable (e.g., “A
 582 true diffusion coefficient of 1.1×10^{-3} mm²/s is represented by an ADC map pixel/ROI value on the analysis
 583 workstation as 1100.”). DICOM Parametric Map object [111] should be considered for storage of ADC
 584 maps, as it provides unambiguous encoding of the quantity, units, *b*-values used and derivation method used
 585 for ADC calculation [112]. The use of DICOM Parametric Map can facilitate interoperable and standardized
 586 description of the DWI analysis results. It is noted that this object type is a recent introduction to the DICOM
 587 standard and is not widely adopted among the vendors [111, 112].

588 For image QA and protocol optimization, it is preferable to have full *b*-matrix values and diffusion encoding
 589 times provided by the vendors, so that they may be recorded in the appropriate fields in the DICOM file
 590 and reflected in the vendor DICOM conformance statement.

591 3.12.2 SPECIFICATION

592

Parameter	Actor	Requirement
Trace DWI	Scanner Operator/ Image Analyst	All trace DWI at each acquired <i>b</i> -value shall be stored in local PACS and distributed to image analysis workstation(s)
ADC maps		ADC maps generated on the MRI scanner shall be stored in local PACS and distributed to image analysis workstation(s) with preserved DICOM scale tags. ADC map scale/units and <i>b</i> -values used for generation shall be recorded.
Image DICOM		DICOM tags essential for downstream review and diffusion analysis shall be maintained including, pixel intensity scaling [113], <i>b</i> -value, and DWI directionality vs. trace, and ADC scale and units. Trace DWI DICOM at each acquired <i>b</i> -value shall be archived in the local PACS.

593

594 **3.13. Image Analysis**

595 This activity describes criteria and procedures related to producing quantitative measurements from the
 596 images that are necessary to reliably meet the Profile Claim.

597 3.13.1 DISCUSSION

598 ADC maps used for offline image analysis must be equivalent to ADC maps generated on the MRI system.
 599 That is, all software elements (here referred to as “Image Analysis Tool”) including the image
 600 handling/network chain must appropriately deal with potential DICOM scaling of DWI and ADC pixel
 601 values [113] and fit algorithm bias, otherwise quantitative content may be lost. The level of “equivalence”
 602 is expected to be well within the ROI standard deviation. Discrepancy comparable to or greater than the
 603 standard deviation suggests erroneous scaling of the ADC map by the image analysis software, possibly
 604 due to incorrect or missing DICOM information. Any such discrepancy must be resolved before proceeding
 605 with statistical analysis for profile compliance.

606

607 When the image analysis software is used to generate ADC maps from source DWI, the software must use
 608 a mono exponential model of DWI signal versus *b*-value. Offline image analysis software must be able to
 609 extract *b*-value and diffusion axis direction content from the DICOM header to appropriately derive ADC
 610 maps (e.g., from isotropic or trace DWI). The resulting ADC maps should also have associated scale and
 611 unit meta-data saved for quantitative analysis. The numerical software conformance and signal-to-noise
 612 sensitivity (bias and range linearity with respect to ground-truth ADC values) can be tested over the range
 613 of *b*-values and tissue-like ADC using the DWI digital reference object [100], available on the QIDW

614 (<https://bit.ly/2QXLo3e>). The choice of fit algorithm (log-linear vs. a non-linear exponential model) can
 615 also be informed by DWI DRO analysis to minimize noise-induced errors and biases.

616
 617 For longitudinal analysis, level and range of slices with tissue/tumor of interest should be reasonably
 618 matched each time the measurements are performed. Ancillary MR images (e.g., high b -value DWI, T_1 -
 619 weighted, T_2 -weighted, post-gadolinium) that best contrast the lesion of interest, can aid ROI placement
 620 [21, 67, 68] on ADC maps. Tissue or lesion ADC quantification requires ROI delineation in two or three-
 621 dimensions. Ideally, ROI geometry is retained for future reference. The ROI is chosen by the radiologist to
 622 match the same lesion/tissue assayed on prior time points, though the ROI size may change in longitudinal
 623 imaging of a given lesion due to treatment response or disease progression. Selected ROI size should be
 624 sufficient to represent the targeted ADC statistics. That is, ROIs should be large enough to avoid ADC
 625 values being unduly influenced by random image noise and/or under-sampled regional heterogeneity.
 626 Procedural steps to create and extract quantities from ROIs vary among software packages. At times,
 627 histogram analysis of whole tumor ROIs may be preferable to allow for distinction between predominantly
 628 solid and heterogeneous cystic/necrotic lesions depending on organ systems.

630 **3.13.1.1 Brain**

631 In brain, avoid contamination within the ROI from tissues such as CSF or that may have high iron content,
 632 such as acute or chronic hemorrhagic areas that have anomalous ADC values. The brain may also contain
 633 areas of large necrotic cysts and surgical cavities - these areas should be avoided.

635 **3.13.1.2 Liver**

636 For liver parenchyma evaluation, ROI placement should avoid large vessels or extraneous anomalous ADC
 637 tissue unrelated to target tissue of interest such as cysts or hemangiomas. Comparison of DWI at $b=0$ having
 638 high SNR revealing both vessels and focal lesions, to moderately low b ($< 100 \text{ s/mm}^2$) where vessels are
 639 suppressed can be useful to localize lesions. It is also important when assessing the ADC of liver
 640 parenchyma to avoid the lateral segment of the left lobe, as this area is subject to pulsatile effects from the
 641 heart, leading to bias in high ADC values.

642
 643 For large liver lesions, special consideration should be given to lesion heterogeneity. Avoidance of central
 644 necrosis or cystic degeneration is recommended so that the quantitative assay is limited to areas of solid
 645 tissue/tumor.

647 **3.13.1.3 Prostate**

648 Prostate ROIs should be manually placed on axial images by the radiologist where the tissues of interest
 649 are adequately conspicuous on the DWI, such as high b -value and/or ADC maps, or identifiable guided by
 650 ancillary MR images.

651 **3.13.1.4 Breast**

652 In breast, avoid contamination within the ROI from areas that have anomalous ADC values due to poor fat
 653 suppression, biopsy hemorrhage, necrotic cysts and surgical cavities.

654 **3.13.2 SPECIFICATION**

655

Parameter	Actor	Requirement
ROI Determination	Radiologist / Image Analyst	Shall segment the ROI on ADC maps consistently across time points using the same software / analysis package guided by a fixed set of image contrasts and avoiding artefacts

ROI geometry		<p>Acceptable: Screen-shot(s) documenting ROI placement on ADC maps shall be retained in the subject database for future reference</p> <p>Target: ROI as a binary pixel mask in image coordinates shall be retained in the subject database for future reference</p> <p>Ideal: ROI shall be saved as a DICOM segment object</p>
Image Display		<p>Acceptable / Target: Software shall allow operator-defined ROI analysis of DWI/ADC aided by inspection of ancillary MR contrasts</p> <p>Ideal: Above plus multi view-port display where DWI/ADC and ancillary MR contrasts from the same scan date are displayed side-by-side and geometrically linked per DICOM (e.g., cursor; cross-hair; ROI; automatically replicated in all view-ports); images from different scan date(s) can be displayed side-by-side, though not necessarily geometrically linked; and ROIs/VOIs may include multiple noncontiguous areas on one slice and/or over multiple slices</p>
Analysis Procedure	Image Analysis Tool	<p>Analysis steps, derived metrics and analysis software package shall be held constant for all subjects and serial time points</p>
ADC statistics		<p>Acceptable/Target: Shall allow display and retention of ROI statistics in patient DICOM database (PACS). Statistics shall include: ADC mean, standard deviation, and ROI/VOI area/volume</p> <p>Ideal: ADC pixel histogram, additional statistics for ADC maximum, minimum, explicit inclusion vs. exclusion of “NaNs” or zero-valued pixels shall be retained with the statistics</p>
ADC scaling		<p>ADC maps scale and units shall be recorded. The difference(s) in mean ADC within replicate ROIs defined on the scanner and analysis workstation(s) shall be less than the ROI standard deviation of the ADC.</p>
ADC map storage /metadata		<p>Acceptable/Target: offline generated ADC maps shall be stored in ITK-compatible format (e.g., NIFTI or MHD) with meta-data traceable to original DWI DICOM (and geometry)</p> <p>Ideal: parametric map DICOM</p>
Fit algorithm type		<p>The specific choice of the fit algorithm shall be recorded, held constant within a study and reported with any dissemination of study findings.</p>
Fit algorithm bias		<p>For offline ADC map generation, the mean ADC shall agree with scanner-generated, or DRO ground truth, ADC values to within one ROI standard deviation.</p>
<i>b</i> -value and direction		<p>Software shall extract <i>b</i>-values and diffusion axis direction from DICOM header</p>

657 4. Assessment Procedures

658 Most of the requirements described in Section 3 can be assessed for conformance by direct observation,
659 however some of the performance-oriented requirements are assessed using a procedure. When a specific
660 assessment procedure is required or to provide clarity, those procedures are defined in subsections here in
661 Section 4 and the subsection is referenced from the corresponding requirement in Section 3.

662 4.1. Assessment Procedure: ADC bias and precision

663 To satisfy site qualification specs for multi-site trial (3.2.2), the baseline ADC measurement bias and
664 precision [30, 34-36] (Appendix E.1) for a given MRI system will be assessed near isocenter using a
665 quantitative DWI phantom. This phantom should contain media with known diffusion properties, similar
666 to ice water-based DWI phantoms [60, 61, 114] or the QIBA DWI phantom [63]. Details for preparation
667 and use of the QIBA DWI phantom are available in the QIBA DWI wiki. “QibaPhanR1.4” software
668 provided through the QIDW can be used to generate the relevant assessment metrics. The assessment
669 procedure is described in detail in Appendix E.1, and will include the following steps:

- 670 • Preparation of temperature controlled DWI phantom to allow sufficient time for the sample to
671 achieve thermal equilibrium (≥ 1 hour) and maintain during scanning (~ 1 hr).
- 672 • Implementation of the system-specific scan protocol including the DWI scan parameters defined in
673 Appendix D, Table D.1.
- 674 • Defining the “Patient Landmark” on the center of the phantom and keeping the prescription of slices
675 centered on Superior/Inferior=0 mm (for horizontal bore magnets).
- 676 • Acquisition of DWI scans according to pre-built protocol and exporting generated trace-DWI
677 DICOM preserving the required metadata for protocol compliance check.
- 678 • Loading DWI DICOM into the image analysis SW and checking compliance of the header metadata
679 with the allowed scan parameter ranges.
- 680 • Calculation of corresponding ADC maps using mono-exponential signal decay model between
681 available pairs of b -values, according to $ADC_{bmin,b} = \frac{1}{(b-bmin)} \ln \left[\frac{S_{bmin}}{S_b} \right]$
- 682 • Defining 1-2 cm ROI (> 80 pixels) with minimal offset from isocenter on ADC images with uniform
683 signal, avoiding artefacts and edges.
- 684 • Estimation of mean ADC bias (BS_{ADC}) in respect to true diffusion constant (DC_{true}) of the phantom
685 medium and confidence interval within ROI containing N pixels with $mean(ADC) = \mu$ and standard
686 deviation $SD(ADC) = \sigma$: $BS_{ADC} \pm CI = (\mu - DC_{true}) \pm 1.96 \frac{\sigma}{\sqrt{N}}$
- 687 • Estimation of the random measurement error (precision) within ROI as: $\%CV = 100\% \cdot \frac{\sigma}{\mu}$
- 688 • Estimation of baseline short-term intra-scan repeatability (RC) and wCV of mean ADC
689 measurement from sequential DWI phantom scans (per scan protocol) based on σ_w^2 intra-scan ADC
690 variance, as: $RC = 2.77 \cdot \sigma_w$; $wCV = 100\% \frac{\sigma_w}{\mu}$
- 691 • Estimation of long-term system repeatability and precision using above-mentioned formalism across
692 multiple longitudinal (periodic QA) phantom scans

693 4.2. Assessment Procedure: Voxel SNR

694 To ensure that relative system performance metric satisfies qualification requirements (3.2.2) and confirm
695 that DWI SNR was adequate to measure ADC bias without incremental bias due to low SNR [92-94]
696 (Appendix E.2) the following assessment steps [115-118] should be followed:

- 697 • Export and combine sequential DWI scans for the quantitative diffusion phantom at fixed b -value

to calculate the temporal (i.e. over the “n” sequential scans) mean of DWI pixel images (“signal image”) and temporal DWI pixel standard deviation images (“temporal noise image”) for each *b*-value.

- When $n=2k$ ($k=1..p$ “pairs” of image sets), “temporal noise image” can be estimated by “DIFF image” = sumODD – sumEVEN, where sum all odd-numbered DWI dynamics called “sumODD image” and sum all even-numbered dynamics called “sumEVEN image”.
- For the isocenter ROIs (1-2 cm diam, >80 pixels), estimate signal-to-noise ratio *n*-scan (SNR_n) according to:

$$SNR_n = \frac{\text{Spatial mean pixel value on Signal Image}}{\text{Spatial mean pixel value on Temporal Noise Image}} \quad \text{or alternatively,}$$

$$altSNR_n = \sqrt{n} \frac{\text{Spatial mean pixel value on Signal Image}}{\text{Spatial standard deviation pixel value on DIFF Image}}$$

- Estimate $CI_{95\%}(SNR_n) = 1.96 \frac{\sigma_{SNR}}{\sqrt{N}}$, using error propagation estimate for $SD(SNR_n)$ by $\sigma_{SNR} = SNR_n \sqrt{sCV^2 + nCV^2}$ with spatial coefficients of variance across *N*-pixel ROI ($N>50$), *sCV* and *nCV*, for the “signal image” and “noise image”, respectively.
- Similar $SNR \pm CI$ estimates can be obtained for the derived multi-scan ADC maps.
- When multiple sequential scans are not available, crudely (subject to Rician bias and background regularization) estimate “noise” level by SD in signal-free background ROI or within the isocenter ROI defined on uniform signal-producing area, and calculate background SNR estimate as:

$$SNR_{vs\ bkgnd} = \frac{\text{Spatial mean pixel value on Signal Image}}{\text{Spatial standard deviation pixel value in background ROI}}$$

- Use above noise estimates for *b*-value CNR calculation, when “signal image” is defined as a difference between pair of (different) *b*-value DWIs.

4.3. Assessment Procedure: ADC *b*-value Dependence

To assess whether an MRI system exhibits artefactual *b*-value dependence in ADC measurement (Appendix E.3) and to satisfy linearity qualification requirements (3.2.2) for this Profile, the assessor will use the following procedure with quantitative diffusion phantom DWI:

- Calculate ADC maps between available pairs of *b*-values, according to $ADC_{b_{min},b} = \frac{1}{(b-b_{min})} \ln \left[\frac{S_{b_{min}}}{S_b} \right]$
- Compare ADC values measured for isocenter ROI for $b_2 \neq b_1$ pairs, using both $(b_1 - b_{min})$ and $(b_2 - b_{min}) \geq 400$ s/mm², as: $ADC\ bvalue\ dependence = 100\% \left\| \frac{(ADC_{b_{min},b_2} - ADC_{b_{min},b_1})}{ADC_{b_{min},b_1}} \right\|$

4.4. Assessment Procedure: ADC Spatial Bias

To assess spatial uniformity of diffusion weighting [61, 119] in respect to nominal *b*-value at isocenter and to meet baseline qualification specs (3.2.2, Appendix E.4) for specific study protocol:

- Select uniform quantitative DWI phantom with known, or measured at isocenter, ADC value and geometry that spans the imaging volume for the studied organ and fits in the application-specific receiver coil
- Perform DWI phantom scans including locations offset from isocenter and derive ADC maps.
- Define multiple ROIs offset from isocenter and spanning the imaged volume, and map the offset-dependence for the mean ADC values.
- Calculate ADC bias with respect to known phantom value as a function of the offset from isocenter.
- Compare the measured bias with the maximum allowed by specifications in Section 3.2.2.

4.5. Assessment Procedure: Image Analysis Software

738 This procedure assesses the ability of analysis SW to properly interpret quantitative header metadata (image
739 scaling, *b*-value and directionality, Section 3.13) and the fidelity of the DWI fitting algorithm to yield
740 unbiased ADC estimate in presence of Rician noise (e.g., Appendix E.2, Figure E.1).

- 741 • For the phantom or subject with known “reference” ADC, generate ADC maps and ROI
742 measurements (e.g., mean and SD for ADC over a 1cm circular ROI) on the scanner console and
743 save the screen-capture
- 744 • Replicate the ROI placement on the images loaded to off-scanner analysis SW and confirm
745 equivalence of displayed values and units to the on-scanner reference values.
- 746 • Load acquired reference DWI DICOM into offline analysis SW and derive ADC maps using the fit
747 algorithm of choice. Compare offline ADC mean and SD to the on-scanner reference ROI ADC
748 value
- 749 • Load DWI DRO DICOM (e.g., provided by QIDW) into the analysis SW and derive ADC maps
750 using the fit algorithm of choice (e.g., non-linear exponential, or log-intensity linear fit).
- 751 • Compare derived parametric ADC maps with known DRO input to estimate bias and SD with
752 respect to true values as a function of SNR and ADC over the ranges relevant for the specific organs.
753

754 **References**

- 755 1. Baehring, J.M. and R.K. Fulbright, *Diffusion-weighted MRI in neuro-oncology*. CNS Oncol, 2012.
756 **1**(2): p. 155-67.
- 757 2. Barboriak, D.P., *Imaging of brain tumors with diffusion-weighted and diffusion tensor MR imaging*.
758 Magn Reson Imaging Clin N Am, 2003. **11**(3): p. 379-401.
- 759 3. Chenevert, T.L., et al., *Diffusion MRI: a new strategy for assessment of cancer therapeutic efficacy*.
760 Mol Imaging, 2002. **1**(4): p. 336-43.
- 761 4. deSouza, N.M., A. Rockall, and S. Freeman, *Functional MR Imaging in Gynecologic Cancer*. Magn
762 Reson Imaging Clin N Am, 2016. **24**(1): p. 205-22.
- 763 5. Galban, S., et al., *Diffusion-weighted MRI for assessment of early cancer treatment response*. Curr
764 Pharm Biotechnol, 2010. **11**(6): p. 701-8.
- 765 6. Gao, X., et al., *Magnetic resonance imaging in assessment of treatment response of gamma knife*
766 *for brain tumors*. Chin Med J (Engl), 2011. **124**(12): p. 1906-10.
- 767 7. Garcia-Figueiras, R., A.R. Padhani, and S. Baleato-Gonzalez, *Therapy Monitoring with Functional*
768 *and Molecular MR Imaging*. Magn Reson Imaging Clin N Am, 2016. **24**(1): p. 261-88.
- 769 8. Higano, S., et al., *Malignant astrocytic tumors: clinical importance of apparent diffusion coefficient*
770 *in prediction of grade and prognosis*. Radiology, 2006. **241**(3): p. 839-46.
- 771 9. Kang, Y., et al., *Gliomas: Histogram analysis of apparent diffusion coefficient maps with standard-*
772 *or high-b-value diffusion-weighted MR imaging--correlation with tumor grade*. Radiology, 2011.
773 **261**(3): p. 882-90.
- 774 10. Kim, M. and H.S. Kim, *Emerging Techniques in Brain Tumor Imaging: What Radiologists Need to*
775 *Know*. Korean J Radiol, 2016. **17**(5): p. 598-619.
- 776 11. Kim, S., et al., *Diffusion-weighted magnetic resonance imaging for predicting and detecting early*
777 *response to chemoradiation therapy of squamous cell carcinomas of the head and neck*. Clin Cancer
778 Res, 2009. **15**(3): p. 986-94.
- 779 12. Koh, D.M., et al., *Body Diffusion-weighted MR Imaging in Oncology: Imaging at 3 T*. Magn Reson
780 Imaging Clin N Am, 2016. **24**(1): p. 31-44.
- 781 13. Lupo, J.M. and S.J. Nelson, *Advanced magnetic resonance imaging methods for planning and*
782 *monitoring radiation therapy in patients with high-grade glioma*. Semin Radiat Oncol, 2014. **24**(4):
783 p. 248-58.
- 784 14. Maier, S.E., Y. Sun, and R.V. Mulkern, *Diffusion imaging of brain tumors*. NMR Biomed, 2010. **23**(7):
785 p. 849-64.
- 786 15. Murakami, R., et al., *Grading astrocytic tumors by using apparent diffusion coefficient parameters:*
787 *superiority of a one- versus two-parameter pilot method*. Radiology, 2009. **251**(3): p. 838-45.
- 788 16. Nelson, S.J., *Assessment of therapeutic response and treatment planning for brain tumors using*
789 *metabolic and physiological MRI*. NMR Biomed, 2011. **24**(6): p. 734-49.
- 790 17. Padhani, A.R., *Diffusion magnetic resonance imaging in cancer patient management*. Semin Radiat
791 Oncol, 2011. **21**(2): p. 119-40.
- 792 18. Padhani, A.R. and A. Gogbashian, *Bony metastases: assessing response to therapy with whole-body*
793 *diffusion MRI*. Cancer Imaging, 2011. **11 Spec No A**: p. S129-45.
- 794 19. Padhani, A.R. and D.M. Koh, *Diffusion MR imaging for monitoring of treatment response*. Magn
795 Reson Imaging Clin N Am, 2011. **19**(1): p. 181-209.
- 796 20. Padhani, A.R., D.M. Koh, and D.J. Collins, *Whole-body diffusion-weighted MR imaging in cancer:*
797 *current status and research directions*. Radiology, 2011. **261**(3): p. 700-18.
- 798 21. Padhani, A.R., et al., *Diffusion-weighted magnetic resonance imaging as a cancer biomarker:*

- 799 *consensus and recommendations*. *Neoplasia*, 2009. **11**(2): p. 102-25.
- 800 22. Patterson, D.M., A.R. Padhani, and D.J. Collins, *Technology insight: water diffusion MRI--a potential*
801 *new biomarker of response to cancer therapy*. *Nat Clin Pract Oncol*, 2008. **5**(4): p. 220-33.
- 802 23. Pope, W.B., et al., *Recurrent glioblastoma multiforme: ADC histogram analysis predicts response*
803 *to bevacizumab treatment*. *Radiology*, 2009. **252**(1): p. 182-9.
- 804 24. Provenzale, J.M., S. Mukundan, and D.P. Barboriak, *Diffusion-weighted and perfusion MR imaging*
805 *for brain tumor characterization and assessment of treatment response*. *Radiology*, 2006. **239**(3):
806 p. 632-49.
- 807 25. Rosenkrantz, A.B., et al., *Body diffusion kurtosis imaging: Basic principles, applications, and*
808 *considerations for clinical practice*. *J Magn Reson Imaging*, 2015. **42**(5): p. 1190-202.
- 809 26. Schmainda, K.M., *Diffusion-weighted MRI as a biomarker for treatment response in glioma*. *CNS*
810 *Oncol*, 2012. **1**(2): p. 169-80.
- 811 27. Shiroishi, M.S., J.L. Boxerman, and W.B. Pope, *Physiologic MRI for assessment of response to*
812 *therapy and prognosis in glioblastoma*. *Neuro Oncol*, 2016. **18**(4): p. 467-78.
- 813 28. Taouli, B. and D.M. Koh, *Diffusion-weighted MR imaging of the liver*. *Radiology*, 2010. **254**(1): p.
814 47-66.
- 815 29. Yamasaki, F., et al., *Apparent diffusion coefficient of human brain tumors at MR imaging*.
816 *Radiology*, 2005. **235**(3): p. 985-91.
- 817 30. Barnhart, H.X. and D.P. Barboriak, *Applications of the repeatability of quantitative imaging*
818 *biomarkers: a review of statistical analysis of repeat data sets*. *Transl Oncol*, 2009. **2**(4): p. 231-5.
- 819 31. Goldmacher, G.V., et al., *Standardized Brain Tumor Imaging Protocol for Clinical Trials*. *AJNR Am J*
820 *Neuroradiol*, 2015. **36**(10): p. E65-6.
- 821 32. Jackson, E.F., et al., *Magnetic resonance assessment of response to therapy: tumor change*
822 *measurement, truth data and error sources*. *Transl Oncol*, 2009. **2**(4): p. 211-5.
- 823 33. Meyer, C.R., et al., *Quantitative imaging to assess tumor response to therapy: common themes of*
824 *measurement, truth data, and error sources*. *Transl Oncol*, 2009. **2**(4): p. 198-210.
- 825 34. Obuchowski, N.A., et al., *Statistical Issues in Testing Conformance with the Quantitative Imaging*
826 *Biomarker Alliance (QIBA) Profile Claims*. *Acad Radiol*, 2016. **23**(4): p. 496-506.
- 827 35. Obuchowski, N.A., et al., *Quantitative imaging biomarkers: a review of statistical methods for*
828 *computer algorithm comparisons*. *Stat Methods Med Res*, 2015. **24**(1): p. 68-106.
- 829 36. Raunig, D.L., et al., *Quantitative imaging biomarkers: a review of statistical methods for technical*
830 *performance assessment*. *Stat Methods Med Res*, 2015. **24**(1): p. 27-67.
- 831 37. Sullivan, D.C., et al., *Metrology Standards for Quantitative Imaging Biomarkers*. *Radiology*, 2015.
832 **277**(3): p. 813-25.
- 833 38. Li, S.P. and A.R. Padhani, *Tumor response assessments with diffusion and perfusion MRI*. *J Magn*
834 *Reson Imaging*, 2012. **35**(4): p. 745-63.
- 835 39. O'Connor, J.P., et al., *Imaging biomarker roadmap for cancer studies*. *Nat Rev Clin Oncol*, 2016.
- 836 40. Partridge, S.C., et al., *Diffusion-weighted MRI Findings Predict Pathologic Response in Neoadjuvant*
837 *Treatment of Breast Cancer: The ACRIN 6698 Multicenter Trial*. *Radiology*, 2018. **289**(3): p. 618-
838 627.
- 839 41. Chenevert, T.L., P.C. Sundgren, and B.D. Ross, *Diffusion imaging: insight to cell status and*
840 *cytoarchitecture*. *Neuroimaging Clin N Am*, 2006. **16**(4): p. 619-32, viii-ix.
- 841 42. Ross, B.D., et al., *Evaluation of cancer therapy using diffusion magnetic resonance imaging*. *Mol*
842 *Cancer Ther*, 2003. **2**(6): p. 581-7.
- 843 43. Newitt, D.C., et al., *Test-retest repeatability and reproducibility of ADC measures by breast DWI:*
844 *Results from the ACRIN 6698 trial*. *J Magn Reson Imaging*, 2018.

- 845 44. Sorace, A.G., et al., *Repeatability, reproducibility, and accuracy of quantitative mri of the breast in*
846 *the community radiology setting.* J Magn Reson Imaging, 2018.
- 847 45. Bonekamp, D., et al., *Diffusion tensor imaging in children and adolescents: reproducibility,*
848 *hemispheric, and age-related differences.* Neuroimage, 2007. **34**(2): p. 733-42.
- 849 46. Paldino, M.J., et al., *Repeatability of quantitative parameters derived from diffusion tensor imaging*
850 *in patients with glioblastoma multiforme.* J Magn Reson Imaging, 2009. **29**(5): p. 1199-205.
- 851 47. Pfefferbaum, A., E. Adalsteinsson, and E.V. Sullivan, *Replicability of diffusion tensor imaging*
852 *measurements of fractional anisotropy and trace in brain.* J Magn Reson Imaging, 2003. **18**(4): p.
853 427-33.
- 854 48. Braithwaite, A.C., et al., *Short- and midterm reproducibility of apparent diffusion coefficient*
855 *measurements at 3.0-T diffusion-weighted imaging of the abdomen.* Radiology, 2009. **250**(2): p.
856 459-65.
- 857 49. Deckers, F., et al., *Apparent diffusion coefficient measurements as very early predictive markers of*
858 *response to chemotherapy in hepatic metastasis: a preliminary investigation of reproducibility and*
859 *diagnostic value.* J Magn Reson Imaging, 2014. **40**(2): p. 448-56.
- 860 50. Heijmen, L., et al., *Diffusion-weighted MR imaging in liver metastases of colorectal cancer:*
861 *reproducibility and biological validation.* Eur Radiol, 2013. **23**(3): p. 748-56.
- 862 51. Miquel, M.E., et al., *In vitro and in vivo repeatability of abdominal diffusion-weighted MRI.* Br J
863 Radiol, 2012. **85**(1019): p. 1507-12.
- 864 52. Gibbs, P., Pickles, M.D., L.W. Turnbull, *Repeatability of echo-planar-based diffusion measurements*
865 *of the human prostate at 3T.* Magn Reson Imaging, 2007. **25**(10): p. 1423-9.
- 866 53. Jambor, I., et al., *Optimization of b-value distribution for biexponential diffusion-weighted MR*
867 *imaging of normal prostate.* J Magn Reson Imaging, 2014. **39**(5): p. 1213-22.
- 868 54. Jambor, I., et al., *Evaluation of different mathematical models for diffusion-weighted imaging of*
869 *normal prostate and prostate cancer using high b-values: a repeatability study.* Magn Reson Med,
870 2015. **73**(5): p. 1988-98.
- 871 55. Litjens, G.J., et al., *Interpatient variation in normal peripheral zone apparent diffusion coefficient:*
872 *effect on the prediction of prostate cancer aggressiveness.* Radiology, 2012. **265**(1): p. 260-6.
- 873 56. Fedorov, A., et al., *Multiparametric MRI of the prostate: repeatability of volume and apparent*
874 *diffusion coefficient quantification.* Invest Radiol, 2017. **52**: p. 538-46.
- 875 57. Afaq, A., et al., *Clinical utility of diffusion-weighted magnetic resonance imaging in prostate cancer.*
876 BJU Int, 2011. **108**(11): p. 1716-22.
- 877 58. Winfield, J.M., et al., *Extracranial Soft-Tissue Tumors: Repeatability of Apparent Diffusion*
878 *Coefficient Estimates from Diffusion-weighted MR Imaging.* Radiology, 2017: p. 161965.
- 879 59. Hegde, J.V., et al., *Multiparametric MRI of prostate cancer: an update on state-of-the-art*
880 *techniques and their performance in detecting and localizing prostate cancer.* J Magn Reson
881 Imaging, 2013. **37**(5): p. 1035-54.
- 882 60. Chenevert, T.L., et al., *Diffusion coefficient measurement using a temperature-controlled fluid for*
883 *quality control in multicenter studies.* J Magn Reson Imaging, 2011. **34**(4): p. 983-7.
- 884 61. Malyarenko, D.I., et al., *Demonstration of nonlinearity bias in the measurement of the apparent*
885 *diffusion coefficient in multicenter trials.* Magn Reson Med, 2016. **75**(3): p. 1312-23.
- 886 62. Pierpaoli, C., et al. *Polyvinylpyrrolidone (PVP) water solutions as isotropic phantoms for diffusion*
887 *MRI studies.* in ISMRM 17th annual meeting. 2009. Honolulu, HI.
- 888 63. Boss, M.A., et al. *Temperature-Controlled Isotropic Diffusion Phantom with Wide Range of*
889 *Apparent Diffusion Coefficients for Multicenter Assessment of Scanner Repeatability and*
890 *Reproducibility.* in *Proceeding of the International Society of Magnetic Resonance in Medicine.*

- 891 2014. Milan, Italy.
- 892 64. Malyarenko, D., et al., *Multi-system repeatability and reproducibility of apparent diffusion*
893 *coefficient measurement using an ice-water phantom*. J Magn Reson Imaging, 2013. **37**(5): p. 1238-
894 46.
- 895 65. Mulkern, R.V., et al., *Pediatric brain tumor consortium multisite assessment of apparent diffusion*
896 *coefficient z-axis variation assessed with an ice-water phantom*. Acad Radiol, 2015. **22**(3): p. 363-
897 9.
- 898 66. Palacios, E.M., et al., *Toward Precision and Reproducibility of Diffusion Tensor Imaging: A*
899 *Multicenter Diffusion Phantom and Traveling Volunteer Study*. AJNR Am J Neuroradiol, 2017. **38**(3):
900 p. 537-545.
- 901 67. Ellingson, B.M., et al., *Diffusion MRI quality control and functional diffusion map results in ACRIN*
902 *6677/RTOG 0625: a multicenter, randomized, phase II trial of bevacizumab and chemotherapy in*
903 *recurrent glioblastoma*. Int J Oncol, 2015. **46**(5): p. 1883-92.
- 904 68. Ellingson, B.M., et al., *Consensus recommendations for a standardized Brain Tumor Imaging*
905 *Protocol in clinical trials*. Neuro Oncol, 2015. **17**(9): p. 1188-98.
- 906 69. Barth, M., et al., *Simultaneous multislice (SMS) imaging techniques*. Magn Reson Med, 2016. **75**(1):
907 p. 63-81.
- 908 70. Eichner, C., et al., *Slice accelerated diffusion-weighted imaging at ultra-high field strength*. Magn
909 Reson Med, 2014. **71**(4): p. 1518-25.
- 910 71. Obele, C.C., et al., *Simultaneous Multislice Accelerated Free-Breathing Diffusion-Weighted Imaging*
911 *of the Liver at 3T*. Abdom Imaging, 2015. **40**(7): p. 2323-30.
- 912 72. Wu, X., et al., *Simultaneous multislice multiband parallel radiofrequency excitation with*
913 *independent slice-specific transmit B1 homogenization*. Magn Reson Med, 2013. **70**(3): p. 630-8.
- 914 73. Hamilton, J., D. Franson, and N. Seiberlich, *Recent advances in parallel imaging for MRI*. Prog Nucl
915 Magn Reson Spectrosc, 2017. **101**: p. 71-95.
- 916 74. Barth, B.K., et al., *Diffusion-Weighted Imaging of the Prostate: Image Quality and Geometric*
917 *Distortion of Readout-Segmented Versus Selective-Excitation Accelerated Acquisitions*. Invest
918 Radiol, 2015. **50**(11): p. 785-91.
- 919 75. Chen, N.K., et al., *A robust multi-shot scan strategy for high-resolution diffusion weighted MRI*
920 *enabled by multiplexed sensitivity-encoding (MUSE)*. Neuroimage, 2013. **72**: p. 41-7.
- 921 76. Setsompop, K., et al., *Improving diffusion MRI using simultaneous multi-slice echo planar imaging*.
922 Neuroimage, 2012. **63**(1): p. 569-80.
- 923 77. Singer, L., et al., *High-resolution diffusion-weighted magnetic resonance imaging in patients with*
924 *locally advanced breast cancer*. Acad Radiol, 2012. **19**(5): p. 526-34.
- 925 78. Wilmes, L.J., et al., *High-resolution diffusion-weighted imaging for monitoring breast cancer*
926 *treatment response*. Acad Radiol, 2013. **20**(5): p. 581-9.
- 927 79. Deng, J., et al., *Multishot diffusion-weighted PROPELLER magnetic resonance imaging of the*
928 *abdomen*. Invest Radiol, 2006. **41**(10): p. 769-75.
- 929 80. Sorensen, A.G., et al., *Hyperacute stroke: evaluation with combined multisection diffusion-*
930 *weighted and hemodynamically weighted echo-planar MR imaging*. Radiology, 1996. **199**(2): p.
931 391-401.
- 932 81. van Gelderen, P., et al., *Water diffusion and acute stroke*. Magn Res Med, 1994. **31**(2): p. 154-63.
- 933 82. Bastin, M.E., *Correction of eddy current-induced artefacts in diffusion tensor imaging using*
934 *iterative cross-correlation*. Magn Reson Imaging, 1999. **17**(7): p. 1011-24.
- 935 83. Le Bihan, D., et al., *Artifacts and pitfalls in diffusion MRI*. J Magn Res Imag, 2006. **24**(3): p. 478-88.
- 936 84. Mohammadi, S., et al., *Correcting eddy current and motion effects by affine whole-brain*

- 937 *registrations: evaluation of three-dimensional distortions and comparison with slice-wise*
 938 *correction.* Magn Reson Med, 2010. **64**(4): p. 1047-56.
- 939 85. Dyvorne, H.A., et al., *Diffusion-weighted imaging of the liver with multiple b values: effect of*
 940 *diffusion gradient polarity and breathing acquisition on image quality and intravoxel incoherent*
 941 *motion parameters--a pilot study.* Radiology, 2013. **266**(3): p. 920-9.
- 942 86. Kakite, S., et al., *Hepatocellular carcinoma: short-term reproducibility of apparent diffusion*
 943 *coefficient and intravoxel incoherent motion parameters at 3.0T.* J Magn Reson Imaging, 2015.
 944 **41**(1): p. 149-56.
- 945 87. LeBihan, D., *IVIM method measures diffusion and perfusion.* Diagn Imaging (San Franc), 1990.
 946 **12**(6): p. 133, 136.
- 947 88. Lee, Y., et al., *Intravoxel incoherent motion diffusion-weighted MR imaging of the liver: effect of*
 948 *triggering methods on regional variability and measurement repeatability of quantitative*
 949 *parameters.* Radiology, 2015. **274**(2): p. 405-15.
- 950 89. Takahara, T. and T.C. Kwee, *Low b-value diffusion-weighted imaging: emerging applications in the*
 951 *body.* J Magn Reson Imaging, 2012. **35**(6): p. 1266-73.
- 952 90. Yoon, J.H., et al., *Evaluation of hepatic fibrosis using intravoxel incoherent motion in diffusion-*
 953 *weighted liver MRI.* J Comput Assist Tomogr, 2014. **38**(1): p. 110-6.
- 954 91. Merisaari, H., et al., *Fitting methods for intravoxel incoherent motion imaging of prostate cancer*
 955 *on region of interest level: Repeatability and gleason score prediction.* Magn Reson Med, 2017.
 956 **77**(3): p. 1249-1264.
- 957 92. Basu, S., T. Fletcher, and R. Whitaker, *Rician noise removal in diffusion tensor MRI.* Med Image
 958 *Comput Comput Assist Interv*, 2006. **9**(Pt 1): p. 117-25.
- 959 93. Kristoffersen, A., *Optimal estimation of the diffusion coefficient from non-averaged and averaged*
 960 *noisy magnitude data.* J Magn Reson, 2007. **187**(2): p. 293-305.
- 961 94. Lui, D., et al., *Monte Carlo bias field correction in endorectal diffusion imaging.* IEEE Trans Biomed
 962 *Eng*, 2014. **61**(2): p. 368-80.
- 963 95. Chen, N.K. and A.M. Wyrwicz, *Removal of EPI Nyquist ghost artifacts with two-dimensional phase*
 964 *correction.* Magn Reson Med, 2004. **51**(6): p. 1247-53.
- 965 96. Guglielmo, F.F., et al., *Hepatic MR imaging techniques, optimization, and artifacts.* Magn Reson
 966 *Imaging Clin N Am*, 2014. **22**(3): p. 263-82.
- 967 97. Koh, D.M., et al., *Whole-body diffusion-weighted MRI: tips, tricks, and pitfalls.* AJR Am J
 968 *Roentgenol*, 2012. **199**(2): p. 252-62.
- 969 98. Kuhl, C.K., et al., *Sensitivity encoding for diffusion-weighted MR imaging at 3.0 T: intraindividual*
 970 *comparative study.* Radiology, 2005. **234**(2): p. 517-26.
- 971 99. Grieve, S.M., A.M. Blamire, and P. Styles, *Elimination of Nyquist ghosting caused by read-out to*
 972 *phase-encode gradient cross-terms in EPI.* Magn Reson Med, 2002. **47**(2): p. 337-43.
- 973 100. Jackson, E.F., et al. *Acceptance Testing and Quality Assurance Procedures for Magnetic Resonance*
 974 *Imaging Facilities, Report of MR Subcommittee Task Group I.* 2010; Available from:
 975 http://www.aapm.org/pubs/reports/RPT_100.pdf.
- 976 101. Reese, T.G., et al., *Reduction of eddy-current-induced distortion in diffusion MRI using a twice-*
 977 *refocused spin echo.* Magn Reson Med, 2003. **49**(1): p. 177-82.
- 978 102. Bendel, P. and Y. Schiftenbauer, *A method for fat suppression in MRI based on diffusion-weighted*
 979 *imaging.* Phys Med Biol, 2010. **55**(22): p. N547-55.
- 980 103. Hansmann, J., D. Hernando, and S.B. Reeder, *Fat confounds the observed apparent diffusion*
 981 *coefficient in patients with hepatic steatosis.* Magn Reson Med, 2013. **69**(2): p. 545-52.
- 982 104. Hernando, D., et al., *Removal of olefinic fat chemical shift artifact in diffusion MRI.* Magn Reson

- 983 Med, 2011. **65**(3): p. 692-701.
- 984 105. Nagy, Z. and N. Weiskopf, *Efficient fat suppression by slice-selection gradient reversal in twice-*
985 *refocused diffusion encoding*. Magn Reson Med, 2008. **60**(5): p. 1256-60.
- 986 106. Sarlls, J.E., et al., *Robust fat suppression at 3T in high-resolution diffusion-weighted single-shot*
987 *echo-planar imaging of human brain*. Magn Reson Med, 2011. **66**(6): p. 1658-65.
- 988 107. Kwee, T.C., et al., *Diffusion-weighted whole-body imaging with background body signal*
989 *suppression (DWIBS): features and potential applications in oncology*. Eur Radiol, 2008. **18**(9): p.
990 1937-52.
- 991 108. Takahara, T., et al., *Diffusion-weighted magnetic resonance imaging of the liver using tracking only*
992 *navigator echo: feasibility study*. Invest Radiol, 2010. **45**(2): p. 57-63.
- 993 109. McRobbie, D.S., Scott, *Quality Control and Artefacts in Magnetic Resonance Imaging*. 2017:
994 Institute of Physics and Engineering in Medicine. 236.
- 995 110. Partridge, S.C., et al., *Diffusion-weighted breast MRI: Clinical applications and emerging*
996 *techniques*. J Magn Reson Imaging, 2017. **45**(2): p. 337-355.
- 997 111. DICOM. *Parametric Map IOD Description*. Available from:
998 http://dicom.nema.org/medical/dicom/current/output/chtml/part03/sect_A.75.html.
- 999 112. NEMA. *ADCmodelparameters*. Available from:
1000 ftp://medical.nema.org/medical/dicom/cp/cp1665_vp_ADCmodelparameters.pdf.
- 1001 113. Chenevert, T.L., et al., *Errors in Quantitative Image Analysis due to Platform-Dependent Image*
1002 *Scaling*. Transl Oncol, 2014. **7**(1): p. 65-71.
- 1003 114. Jerome, N.P., et al., *Development of a temperature-controlled phantom for magnetic resonance*
1004 *quality assurance of diffusion, dynamic, and relaxometry measurements*. Med Phys, 2016. **43**(6):
1005 p. 2998.
- 1006 115. Aja-Fernandez, S., C. Alberola-Lopez, and C.F. Westin, *Noise and signal estimation in magnitude*
1007 *MRI and Rician distributed images: a LMMSE approach*. IEEE Trans Image Process, 2008. **17**(8): p.
1008 1383-98.
- 1009 116. Sijbers, J. and A.J. den Dekker, *Maximum likelihood estimation of signal amplitude and noise*
1010 *variance from MR data*. Magn Reson Med, 2004. **51**(3): p. 586-94.
- 1011 117. Friedman, L. and G.H. Glover, *Report on a multicenter fMRI quality assurance protocol*. J Magn
1012 Reson Imaging, 2006. **23**(6): p. 827-39.
- 1013 118. Dietrich, O., et al., *Measurement of signal-to-noise ratios in MR images: influence of multichannel*
1014 *coils, parallel imaging, and reconstruction filters*. J Magn Reson Imaging, 2007. **26**(2): p. 375-85.
- 1015 119. Bammer, R., et al., *Analysis and generalized correction of the effect of spatial gradient field*
1016 *distortions in diffusion-weighted imaging*. Magn Reson Med, 2003. **50**(3): p. 560-9.
- 1017 120. Malkyarenko, D.I. and T.L. Chenevert, *Practical estimate of gradient nonlinearity for*
1018 *implementation of apparent diffusion coefficient bias correction*. J Magn Reson Imaging, 2014.
1019 **40**(6): p. 1487-95.
- 1020 121. Malyarenko, D.I., et al., *Correction of Gradient Nonlinearity Bias in Quantitative Diffusion*
1021 *Parameters of Renal Tissue with Intra Voxel Incoherent Motion*. Tomography, 2015. **1**(2): p. 145-
1022 151.
- 1023 122. Malyarenko, D.I., B.D. Ross, and T.L. Chenevert, *Analysis and correction of gradient nonlinearity*
1024 *bias in apparent diffusion coefficient measurements*. Magn Reson Med, 2014. **71**(3): p. 1312-23.
- 1025 123. Newitt, D.C., et al., *Gradient nonlinearity correction to improve apparent diffusion coefficient*
1026 *accuracy and standardization in the american college of radiology imaging network 6698 breast*
1027 *cancer trial*. J Magn Reson Imaging, 2015. **42**(4): p. 908-19.

1029 **Appendices**

1030 **Appendix A: Acknowledgements and Attributions**

1031 This document is proffered by the Radiological Society of North America [37], Diffusion-Weighted
1032 Imaging Task Force subgroup of the Perfusion Diffusion and Flow (PDF) Biomarker Committee. The PDF
1033 is composed of scientists, engineers, and clinicians representing academia, the imaging device
1034 manufacturers, image analysis software developers, image analysis laboratories, biopharmaceutical
1035 industry, government research organizations, professional societies, and regulatory agencies, among others.
1036 All work is classified as pre-competitive.

1037 The following individuals have made critical contributions in the development of this Profile:

1038	Rajpaul Attariwala	Chen Lin
1039	Daniel Barboriak	Mikko Määttä
1040	David Bennett	Dariya Malyarenko
1041	Ishtiaq Bercha	Elizabeth Mirowski
1042	Michael Boss	Bastien Moreau
1043	Orest Boyko	David Newitt
1044	Martin Büchert	Nancy Obuchowski
1045	Thomas Chenevert	Estanislao Oubel
1046	Caroline Chung	Savannah Partridge
1047	Amita Shukla Dave	Thorsten Persigehl
1048	Andrey Fedorov	Mark Rosen
1049	Clifton Fuller	Mark Shiroishi
1050	Alexander Guimaraes	Rohit Sood
1051	Marko Ivancevic	Daniel Sullivan
1052	Edward Jackson	Ying Tang
1053	Ivan Jambor	Bachir Taouli
1054	John Kirsch	Aradhana Venkatesan
1055	Daniel Krainak	Lisa Wilmes
1056	Hendrik Laue	Ona Wu
1057	Jiachao Liang	Junqian Xu
1058		Gudrun Zahlmann

1059

1060 We also acknowledge the extraordinary efforts by RSNA QIBA staff in making this Profile possible.

1061

1062 **Appendix B: Background Information**

1063 **QIBA Wiki:**

1064 http://qibawiki.rsna.org/index.php/Main_Page

1065 **QIBA Perfusion, Diffusion, and Flow Biomarker Committee Wiki:**

1066 [http://qibawiki.rsna.org/index.php/Perfusion, Diffusion and Flow-MRI Biomarker Ctte](http://qibawiki.rsna.org/index.php/Perfusion,_Diffusion_and_Flow-MRI_Biomarker_Ctte)

1067 **DWI Literature Review:**

1068 [http://qibawiki.rsna.org/index.php/DWI Literature Review](http://qibawiki.rsna.org/index.php/DWI_Literature_Review)

1069 **QIBAPhan Analysis Software (for ADC and summary statistics of isotropic diffusion phantom):**

1070 <https://bit.ly/2QXLo3e>

1071 **QIBA DWI Digital Reference Object:**

1072 <https://bit.ly/2QXLo3e>

1073 **Diffusion Phantom Preparation and Positioning:**

1074 [http://qibawiki.rsna.org/index.php/Perfusion, Diffusion and Flow-MRI Biomarker Ctte](http://qibawiki.rsna.org/index.php/Perfusion,_Diffusion_and_Flow-MRI_Biomarker_Ctte)

1075 **DICOM MR Diffusion Macro:**

1076 http://dicom.nema.org/medical/dicom/current/output/chtml/part03/sect_C.8.13.5.9.html

1077

1078 **Appendix C: Conventions and Definitions**

1079 **Apparent Diffusion Coefficient (ADC):** A quantitative imaging biomarker (typically in units of mm²/s
 1080 or μm²/ms) indicative of the mobility of water molecules. High ADC indicates free or less hindered mobility
 1081 of water; low ADC indicates slow, restricted, or hindered mobility of water molecules.

1082 **b-value:** An indication of the strength of diffusion-weighting (typically in units of s/mm²). It depends on a
 1083 combination of gradient pulse duration, shape, strength, and the timing between diffusion gradient pulses.

1084 **DICOM:** Digital Imaging and Communications in Medicine standard for distributing and viewing any
 1085 kind of medical image regardless of the origin. A DWI DICOM header typically contains meta-data
 1086 reflecting scan geometry and key acquisition parameters (e.g., b-value and gradient direction) required for
 1087 subsequent generation of ADC maps and ROI statistics. A DWI DICOM macro assigns the required
 1088 diffusion-specific attributes to public DICOM tags (e.g., [0018, 9087], diffusion b-value and [0018, 9075],
 1089 diffusion directionality) which should be available independent of Vendor and scanner software version.
 1090 Currently, vendors do not universally follow the DWI macro standard, storing b-value and direction
 1091 metadata in private tags.

1092 **Diffusion Weighted Image (DWI):** A type of MR image where tissue contrast is dependent on water
 1093 mobility, diffusion gradient direction, concentration of water signal, and T₂ relaxation. On heavily diffusion-
 1094 weighted images (i.e. high b-value), high signal indicates low water mobility, high proton concentration,
 1095 and/or long T₂.

1096 **Isotropic (or trace) DWI:** Directionally-independent diffusion-weighted images obtained as the
 1097 composite (geometric average) of three orthogonal DWIs and used for ADC map derivation. Throughout
 1098 this profile and assessment procedure, the term “DWI” refers to these directionally-independent images
 1099 unless otherwise noted as a specific single-axis or directional DWI. Even in anisotropic media,
 1100 directionally-independent (i.e. scalar) diffusion metrics are measurable using DWI combined from three-
 1101 orthogonal diffusion gradient acquisitions.

1102 **Linearity:** A requirement of a linear relationship between the measured ADC value and the true value over
 1103 a physiologically-relevant range; the slope of this line should be equal to 1.

1104 Ideally, to establish linearity with slope equal to 1, five truth values will be assessed, each with five
 1105 repetitions. The slope may then be assessed by the following procedure:

1106
 1107 For each case, calculate the ADC (denoted Y_i), where i denotes the i-th case. Let X_i denote
 1108 the true value for the i-th case. Fit an ordinary least squares (OLS) regression of the Y_i's on
 1109 X_i's. A quadratic term is first included in the model to rule out non-linear relationships: $Y = \beta_0 + \beta_1 X + \beta_2 X^2$.
 1110 If $|\beta_2| < 0.5$, then a linear model should be fit: $Y = \beta_0 + \beta_1 X$, and R²
 1111 estimated. Let $\widehat{\beta}_1$ denote the estimated slope. Calculate its variance as $\widehat{Var}_{\beta_1} =$
 1112 $\{\sum_{i=1}^N (Y_i - \widehat{Y}_i)^2 / (N - 2)\} / \sum_{i=1}^N (X_i - \bar{X})^2$, where \widehat{Y}_i is the fitted value of Y_i from the
 1113 regression line and \bar{X} is the mean of the true values. The 95% CI for the slope is $\widehat{\beta}_1 \pm$

1114
$$t_{\alpha=0.025, (N-2)df} \sqrt{\widehat{Var}_{\beta_1}}.$$

1115
 1116 The absolute value of the estimate of β₂ should be <0.50 and R-squared (R²) should be
 1117 >0.90. The 95% CI for the slope should be completely contained in the interval 0.95 to 1.05.
 1118

1119 **Repeatability Coefficient (RC):** Represents measurement precision where conditions of the measurement
 1120 procedure (scanner, acquisition parameters, slice locations, image reconstruction, operator, and analysis)
 1121 are held constant over a “short interval”.

1122 **Within-subject Coefficient of Variance (wCV):** Is often reported for repeatability studies to assess
 1123 repeatability in test–retest designs. Calculated as seen in the table below:

1124 **Steps for Calculating the test-retest wCV**

1	Calculate the mean (M) and variance (V) for each of N subjects from their replicate measurements, m1 and m2: $M=(m1+m2)/2$; $V=(m1-m2)^2/2$
2	Calculate the wCV^2 for each of the N subjects by dividing their variance by their mean squared, V/M^2
3	Take the mean of the wCV^2 over the N subjects.
4	Take the square root of the value in step 3 to get an estimate of the wCV.

1125

1126 **Appendix D: Platform-Specific Acquisition Parameters for DWI Phantom Scans**

1127 For acquisition modalities, reconstruction software and software analysis tools, profile conformance
 1128 requires meeting the activity specifications and assessment requirements above in Sections 2, 3 and 4.

1129 This Appendix provides specific acquisition parameters, reconstruction parameters and analysis software
 1130 parameters that are expected to achieve compatibility with profile requirements for technical assessment of
 1131 MRI systems. Just using these parameters without meeting the requirements specified in the profile is not
 1132 sufficient to achieve conformance. Conversely, it is possible to use different compatible parameters and still
 1133 achieve conformance. System operation within provided conformance limits suggests the technical
 1134 contribution to variance does not unduly alter wCV observed in biological measurements. Technical DWI
 1135 performance of a given MRI system relative to peer systems can be assessed using the described
 1136 standardized acquisition protocols designed for existing ice-water DWI phantoms. Platform-specific
 1137 protocols were excerpted from the QIBA ice water-based DWI Phantom scan procedure for axial
 1138 acquisitions. The full QIBA DWI Phantom scan procedure involves acquisitions for coronal, axial and
 1139 sagittal planes as detailed in the QIBA DWI wiki.

1140 Sites using MRI system models listed here are encouraged to consider using parameter settings provided in
 1141 this Profile for both simplicity and consistency of periodic quantitative DWI QA procedures. Sites using
 1142 models not listed here may be able to devise their own settings that result in data meeting the requirements
 1143 of this Profile (at the minimum) or tighter requirements of specific clinical trial.

1144 **IMPORTANT: The presence of a product model/version in these tables does not imply it has**
 1145 **demonstrated conformance with the QIBA Profile. Refer to the QIBA Conformance Statement for**
 1146 **the product.**

1147
1148

Table D.1 Model-specific Parameters for Acquisition Devices When Scanning DWI Phantoms

Acquisition Device	Settings Compatible with Conformance		
Philips	<i>Submitted by: University of Michigan, Department of Radiology</i>		
	Model / Version	Achieva / 5.1.7	Ingenia / 5.1.7
	Field Strength	1.5T	3T
	Receiver Coil	≥8ch head	≥ 15ch head
	Uniformity	CLEAR=yes; Body-Tuned=no	CLEAR = yes
	Slice Orientation	Transaxial	Transaxial
	FOV	220mm	220mm
	Acquisition Voxel Size	1.72x1.72x4mm	1.72x1.72x4mm
	Acquisition Matrix [†]	128x126	128x128
	Recon Voxel Size	0.898x0.898x4mm	0.898x0.898x4mm
	Recon Matrix	256x256	256x256
	SENSE (parallel imaging)	Yes, factor=2	Yes, factor=2
	Fold-over Direction	AP	AP
	Fat-shift direction	P	P
	Foldover-sup / Oversampling	No	No
	Qty Slices	25	25
	Stacks and Packages	1	1
	Slice Thickness	4mm	4mm
	Slice gap (user-defined)	1mm	1mm
	Shim	Volume set to encompass phantom	Vol or PB-Vol to encompass phantom
	B1 shim	Not Applicable	Fixed
	Scan Mode	MS	MS
	Technique	SE	SE
	Acquisition Mode	Cartesian	Cartesian
	Fast Imaging Mode	EPI	EPI
	Shot Mode	Single-shot	Single-shot
	Echoes	1	1
	Partial Echo	No	No
	TE	Shortest (<110ms)	Shortest (<110ms)
	Flip Angle	90°	90°
	TR	10,000ms	10,000ms
	Halfscan factor	≥0.62	≥0.62
	Water-Fat shift (in phase dir)	Minimum (~11xAcqVoxel size)	Minimum (~24xAcqVoxel size)
	Fat suppression	No	No
	Diffusion Mode	DWI	DWI
	Direction	“M,P,S” (i.e. non-Overplus)	“M,P,S” (i.e. non-Overplus)
<i>b</i> -values (user-defined)	0, 500, 900, 2000	0, 500, 900, 2000	
Average high <i>b</i> -values	No	No	
PNS Mode	High	High	
Gradient Mode	Maximum	Maximum	
NSA (averages)	1	1	
Images	M (magnitude)	M (magnitude)	
Preparation phases	Full for 1 st scan; Auto for scan 2,3,4	Full for 1 st scan; Auto for scan 2,3,4	
EPI 2D Phase Correction	No	No	
Save Raw Data	No	No	

1149

Geometry Correction	Default	Default
EPI Factor	67	67
Bandwidth in Freq-direction	1534 Hz	1414 Hz
Scan Duration	~2min/scan; 4scans for ~8min total	~2min/scan; 4scans for ~8min total

† Matrix size can be 128x128 ± 3

Acquisition Device	Settings Compatible with Conformance		
Siemens	<i>Submitted by: Siemens Healthcare</i>		
	Model / Version	Magnetom Aera / VD13	Magnetom Skyra/ VD13
	Field Strength	1.5T	3T
	Receiver Coil	<u>HE1-4</u>	<u>HE1-4</u>
	Slice Orientation	Transaxial	Transaxial
	FOV read and phase	220mm	220mm
	Base resolution	130	130
	Phase resolution	100%	100%
	Recon Voxel Size	0.8x0.8x4mm	0.8x0.8x4mm
	PAT Mode	GRAPPA, PE factor=2	GRAPPA, PE factor=2
	Phase enc Direction	A >> P	A >> P
	Ref lines PE	40	40
	Reference scan mode	Separate	Separate
	Qty Slices	25	25
	Phase oversampling	0%	0%
	Slice Thickness	4mm	4mm
	Distance Factor	25%	25%
	Shim mode	Standard	Standard
	Mode	2D	2D
	Multi-slice mode	Interleaved	Interleaved
	EPI factor	130	130
	Free Echo Spacing	Off	Off
	Echo spacing	0.77ms	0.94ms
	TE	98ms	104ms
	TR	10,000ms	10,000ms
	Fat suppression	No	No
	Diffusion Mode	Orthogonal	Orthogonal
	Diff. weightings	4	4
	b-value 1,2,3,4	0, 500, 900, 2000	0, 500, 900, 2000
	Diff. weighted images	On	On
	Trace weighted images	On	On
	Gradient Mode	Fast	Fast
	Averages	1	1
	Averaging mode	Long term	Long term
Concatenations	1	1	
MTC	Off	Off	
Magn. preparation	None	None	
Filter	DistortionCorr(2D); PrescanNormalize	DistortionCorr(2D); PrescanNormalize	
Reconstruction	Magnitude	Magnitude	
Bandwidth	1538 Hz/Px	1424 Hz/Px	
RF pulse type	Normal	Normal	
Scan Duration	~2min/scan; 4scans for ~8min total	~2min/scan; 4scans for ~8min total	

1150

Acquisition Device	Settings Compatible with Conformance		
General Electric	<i>Submitted by: Memorial Sloan Kettering Cancer Center; and GE Healthcare</i>		
	Model / Version	Optima MR 450 / DV23.1	Discovery MR 750 / DV23.1
	Field Strength	1.5T	3T
	Receiver Coil	<u>8HRBrain</u>	<u>8HRBrain</u>
	Slice Orientation	Transaxial	Transaxial
	FOV	22cm	22cm
	Phase FOV	100%	100%
	Acquisition matrix	128x128	128x128
	Acq voxel size	1.72x1.72x4mm	1.72x1.72x4mm
	Recon voxel size	0.98x0.98x4mm	0.98x0.98x4mm
	ASSET Acceleration, Phase	2	2
	Freq enc. Direction	R/L	R/L
	Qty Slices	25	25
	Slice Thickness	4mm	4mm
	Slice spacing	1mm	1mm
	Shim	Auto	Auto
	Imaging Options	2D, spin-echo, EPI, DIFF	2D, spin-echo, EPI, DIFF
	Num Shots	1	1
	Dual Spin Echo	No	No
	TE	Min Full (~123ms)	Min Full (~104ms)
	TR	10,000ms	10,000ms
	Fat suppression	No	No
	Diffusion Direction	ALL	ALL
	b-value	0, 500, 900, 2000	0, 500, 900, 2000
	Phase Correct	On	On
	dB/dt control mode	1 st	1 st
	NEX	1	1
	Bandwidth	Default (250kHz)	Default (250kHz)
3D Geometry correction	No	No	
Scan Duration	~2min/scan; 4scans for ~8min total	~2min/scan; 4scans for ~8min total	

1151

Acquisition Device	Settings Compatible with Conformance		
Canon	<i>Submitted by: Canon Medical Systems</i>		
	Model/Version	Elan / 4.0SP0003	Galan / 4.0SP0004
	Field Strength	1.5T	3T
	Receiver Coil	Octave head/neck coil	16 or 32-ch head/neck coil
	Slice Orientation	Transaxial	Transaxial
	FOV	22 cm x 22 cm	22 cm x 22 cm
	Matrix Size	128 x 128	128 x 128
	No Wrap	1	1
	SPEEDER Acceleration, Phase	2	2
	Phase Encode	AP	AP
	Number of TE-echoes	16	16

Qty Slices	25	25
Slice Thickness	4 mm	4 mm
Slice Spacing	1 mm	1 mm
Sequence	SEEP12D	SEEP12D
Number of Shots	1	1
Segmentation Type	Sequential	Sequential
TE	110 ms	104 ms
TR	10,000 ms	10,000 ms
Fat Suppression	Off	Off
Diffusion Direction	3-axis	3-axis
<i>b</i> -value	0, 500, 900, 2000	0, 500, 900, 2000
Phase Correction	Type 2 (EPI Nyquist Ghosting)	Type 2 (EPI Nyquist Ghosting)
NAQ	1	1
Receiver Bandwidth	1563 Hz / pixel	1421 Hz / pixel
RF Type	Normal	Normal
GR Type	Fast	Fast
Scan Duration	~2 min/scan	~2 min/scan

1152

1153 **Appendix E: Technical System Performance Evaluation**

1154 Procedures below are for basic evaluation of MRI equipment performance to qualify for quantitative DWI
 1155 trials. Conformance specs for performance metrics (listed in 3.2.2) are suggested to ensure that technical
 1156 measurement errors related to the MRI system do not unduly contribute to measurement variance for subject
 1157 ADC.

1158 **E.1. ADC QUALITIES AT/NEAR ISOCENTER**

1159 To evaluate an MRI system for ADC measurement bias and precision, a phantom containing media having
 1160 known diffusion properties is required. Water maintained at 0 °C is widely used as a known standard with
 1161 diffusion coefficient = $1.10 \times 10^{-3} \text{ mm}^2/\text{s}$, and is the basis for ice water-based DWI phantoms [60, 61, 64,
 1162 114]. This procedure requires access to an ice water DWI phantom, such as the QIBA DWI phantom [62,
 1163 63, 66] or alternative that contains a measurement sample of water ($\geq 30 \text{ mL}$ volume) located at isocenter
 1164 surrounded by an ice water bath [60, 61, 64, 114]. Sufficient time must be allowed for the sample to achieve
 1165 thermal equilibrium ($\geq 1 \text{ hour}$) and the phantom must contain an adequate volume of ice to surround the
 1166 measurement sample over the entire MRI exam period. Details for preparation and use of the QIBA DWI
 1167 phantom are available in the QIBA DWI wiki. The phantom ADC measurement protocol should follow the
 1168 DWI scan parameters defined in Appendix D, Table D.1, which involves DWI acquisition at nominal *b*-
 1169 values = 0, 500, 900, 2000 s/mm^2 .

1170 Typically, MRI systems exhibit best performance at or near isocenter where ADC bias reflects overall
 1171 calibration of gradient amplitude and DWI sequence timing. Proximity to isocenter is to be determined by
 1172 location of the center of an ROI used to assess ADC. Spatial coordinates of the ROI-center are often
 1173 available using the scanner’s electronic caliper read-out of ROI-center coordinates in the patient-based
 1174 frame of reference defined by “Patient Landmark” location. Note, the patient-based frame and magnet-
 1175 based frame (true isocenter) may not be synonymous, and displacement between the two may vary from
 1176 scan series to scan series. To maintain minimal offset between patient-based and magnet-based frames, the
 1177 “Patient Landmark” should be defined on the center of the phantom then the prescription of slices used for
 1178 quantitative evaluation should be kept centered on Superior/Inferior=0 mm (for horizontal bore magnets).
 1179 An ROI having center coordinates [*RL*, *AP*, *SI*] is “at isocenter” when $\sqrt{RL^2 + AP^2 + SI^2} \leq 4 \text{ cm}$, and
 1180 the maximum diameter of the ROI $\leq 2 \text{ cm}$. A minimum ROI diameter of ~1cm will provide sufficient

number of pixels (>80) for adequate sampling of phantom ADC heterogeneity for reliable estimate of within ROI statistics (standard deviation and mean). For uniform analysis, “QibaPhanR1.4” software provided through the QIDW (<https://bit.ly/2pYRrJ6>) can be used to generate the relevant ADC ROI assessment metrics (bias, precision, repeatability and SNR) for QIBA DWI phantom, as described below.

The QIBA DWI phantom, and other water-based phantoms are isotropic so measured diffusion coefficient *should* be independent of applied diffusion gradient direction. Throughout this profile and assessment procedure, “DWI” will refer to the composite of three orthogonal DWIs as the trace DWI.

Two or more diffusion weightings are required to calculate ADC, and full ADC maps are generated on a pixel-by-pixel basis (though low SNR may bias these pixel-by-pixel ADC maps) using the mono-exponential model:

$$ADC_{bmin,b} = \frac{1}{(b-bmin)} \ln \left[\frac{S_{bmin}}{S_b} \right], \quad \text{EQ(1)}$$

where S represents the diffusion weighted image intensity and subscripts refer to b-value. For this assessment procedure, if only two b-values are used, they must include the nominal minimum b-value in the calculation, typically b=0. If all b-values are used in the ADC calculation, a mono-exponential signal decay versus b-value model fit (e.g., least-squares) must be used. To achieve adequate diffusion contrast for ADC estimation via EQ(1), $(b - b_{min})$ should be ≥ 400 s/mm².

The estimate of MRI system ADC bias in measurement of 0°C water ($DC_{true} = 1.1 \times 10^{-3}$ mm²/s [60]) at isocenter should be calculated as:

$$ADC \text{ bias estimate} = \mu - DC_{true}; \text{ or } \%bias = \frac{100\%(\mu - DC_{true})}{DC_{true}}, \quad \text{EQ(2)}$$

where μ is the ROI mean of the ADC map at isocenter and the ROI contains 80-150 pixels. Assuming the pixel values follow a normal distribution, the 95% confidence interval (CI) for this bias estimate is,

$$ADC \text{ bias estimate} \pm 1.96 \frac{\sigma}{\sqrt{N}}, \quad \text{EQ(3)}$$

where σ is the standard deviation of ADC pixel values in the ROI containing N pixels. ADC bias at isocenter allowed by this profile is $|ADC \text{ bias}| \leq 0.04 \times 10^{-3}$ mm²/s.

The standard deviation of ADC pixel values within an isocenter ROI is one indicator of random measurement error (precision) in ADC maps expressed as a percentage relative to the ROI mean (%CV) as:

$$ADC \text{ error estimate} = 100\% \cdot \frac{\sigma}{\mu} \quad \text{EQ(4)}$$

Similar to ADC bias estimate, this procedure typically uses an ROI of ~1 cm² (>80 pixels) on a water sample at 0 °C (e.g., center tube of QIBA DWI phantom) at isocenter, and follow the QIBA DWI phantom scan protocol to estimate ADC error. The random error allowed by this profile specs (3.2.2) is < 2%.

The established QIBA DWI phantom scan protocol is to acquire four DWI scans (each ~2 minutes) in immediate succession holding acquisition conditions constant. This procedure serves multiple aims: (1) inspect for monotonic trend in ADC vs. time suggesting the phantom was not at thermal equilibrium; (2) inspect for artefact or drift suggesting system instability; (3) allow for estimation of voxel signal-to-noise ratio (SNR); and (4) provide an estimate of short-term (intra-exam) repeatability [60, 63-66]. Repeated scanning of the phantom over multiple days/weeks/months more closely resembles serial scanning of patients in longitudinal studies. Regardless of interval over which repeated measurements are performed, assuming normally distributed measures, the Repeatability Coefficient (RC) and “within-subject” Coefficient of Variation as a percentage (wCV) are calculated as [30, 35, 36]:

$$1220 \quad RC = 2.77 \cdot \sigma_w; \quad wCV = 100\% \frac{\sigma_w}{\mu}, \quad EQ(5)$$

1221 where σ_w^2 is the within-subject (phantom) parameter variance (see Appendix C for calculation of the wCV)
 1222 and μ is the parameter mean. The average of repeated ROI means at isocenter and square root of variance
 1223 of these means may be used in EQ(5) to estimate RC and wCV as a metric of system technical performance.
 1224 The allowed short-term and long-term ADC repeatability for this profile are $\leq 1.5 \times 10^{-5} \text{ mm}^2/\text{s}$ and $\leq 6.5 \times$
 1225 $10^{-5} \text{ mm}^2/\text{s}$, respectively [64]. Please note, phantom-based RC and wCV derived here are under relatively
 1226 ideal conditions and should not be taken as representative of repeatability achieved in human DWI/ADC
 1227 studies that involve more sources of variability. The acceptable baseline performance for the device
 1228 assessed with the quantitative DWI phantom and required by this profile to ensure no significant
 1229 contribution to the within-subject RC and CV is summarized in Section 3.2.2.

1230

1231

1232

1233 E.2. DWI SIGNAL TO NOISE

1234 This section describes criteria that are necessary for an MRI system to meet the Profile qualification specs
 1235 listed in 3.2.2. Vendors and imaging sites can use this procedure to estimate relative signal-to-noise ratio
 1236 (SNR) of an MRI system in the context of DWI and parametric ADC maps (both for phantom and subjects).

1237 Signal-to-noise ratio of any MR image is heavily dependent on acquisition conditions so while SNR is
 1238 informative of system performance, its evaluation by the suggested procedure is not an absolute system
 1239 performance metric. Determination of SNR by this procedure serves two aims: (1) provide a relative system
 1240 performance metric; and (2) confirm SNR was adequate to measure ADC bias without incremental bias due
 1241 to low SNR.

1242 This procedure is used to estimate SNR at the acquisition voxel level. Common filtering, interpolation and
 1243 reconstruction algorithms lead to correlated noise in neighboring DWI pixels. Therefore, the described
 1244 procedure relies on analysis that yields a noise estimate averaged over an ROI to mitigate effect of correlated
 1245 noise.

1246 Signal estimated as the mean pixel intensity value over an ROI is straightforward; however, DWI noise
 1247 estimation is more difficult. Using standard deviation of pixel values in signal-free background (i.e. air) as
 1248 noise estimate is unreliable due to commonly-used parallel imaging reconstruction, coil-sensitivity
 1249 equalization routines and Rician bias of “magnitude” signals [92-94, 115, 116, 118]. Instead for this
 1250 procedure, noise will be estimated by the temporal change in pixel values measured over multiple scans.
 1251 The QIBA DWI phantom scan protocol requires four scans repeated in immediate succession holding all
 1252 acquisition conditions constant. Images containing the measurement ROI over these four dynamics should
 1253 be visually inspected for conspicuous (multi-pixel) spatial shift, distortion, or artefact in any of the
 1254 dynamics. Assuming none, random noise is considered to be the main contributor to scan-to-scan
 1255 differences. To assess noise by this procedure, software (similar to “QibaPhanR1.4”) must be available to
 1256 combine dynamic images and calculate the temporal standard deviation of each pixel (i.e., over the “n”
 1257 dynamic scans). An image comprised of the temporal standard deviation of pixel values should be referred
 1258 to as the “temporal noise image”. An image comprised of the temporal mean of pixel values should be
 1259 referred to as the “signal image”. Note, an image comprised of the pixel-by-pixel division of the signal
 1260 image by the temporal noise image is referred to as the “signal-to-fluctuation-noise-ratio image” [117, 118],
 1261 but this should not be used to estimate SNR. Instead, the calculation estimates noise as spatial mean within
 1262 an ROI of temporal noise image and corresponding signal as a spatial ROI mean of the temporal average
 1263 signal image [116]:

1264

$$SNR_{nDyn} = \frac{\text{Spatial mean pixel value on Signal Image}}{\text{Spatial mean pixel value on Temporal Noise Image}} \quad \text{EQ(6)}$$

1265

The 95% confidence interval for this SNR estimate is $\pm 1.96 \frac{\sigma_{SNR}}{\sqrt{N}}$,

1266

where $\sigma_{SNR} = SNR_{nDyn} \sqrt{sCV^2 + nCV^2}$ is the “error propagation” estimate of standard deviation of SNR pixel values in an ROI containing N pixels with spatial coefficients of variance, sCV and nCV , for the temporal average signal image and temporal standard-deviation noise image, respectively.

1267

1268

1269

An alternative procedure to estimate SNR from an even quantity of dynamic scans is to first sum all odd-numbered dynamics called “sumODD image” and sum all even-numbered dynamics called “sumEVEN image”, then create their difference called “DIFF image” = sumODD – sumEVEN. Using these, an estimate of SNR within an ROI from n -dynamic scans acquired in immediate succession holding conditions fixed should be calculated as [117, 118]:

1270

1271

1272

1273

1274

$$altSNR_{nDyn} = \sqrt{n} \frac{\text{Spatial mean pixel value on Signal Image}}{\text{Spatial standard deviation pixel value on DIFF Image}} \quad \text{EQ(7)}$$

1275

EQ(7) should be used when only two dynamic scans ($n=2$) are available.

1276

For conditions defined in this assessment procedure (i.e. 4 dynamics and 80-100 pixel ROIs) equation EQ(6) tends to overestimate SNR slightly although has tighter confidence interval relative to equation EQ(7). The choice of which equation to use may depend on capabilities of the analysis software. SNR analysis via equations EQ(6) and/or EQ(7) may be performed on source DWI images, as well as on derived ADC maps.

1277

1278

1279

1280

In situations where two or more dynamic series are not available, the “noise” level may be crudely estimated (i.e. still subject to Rician bias and background regularization) by the standard deviation in signal-free background or by the standard deviation within the ROI defined on uniform signal-producing area. Prior to defining the background ROI, the assessor should inspect the images with a tight window/level and strive to select a background region that contains uniform random noise while avoiding signal gradients, structured noise (e.g., ghosts) or severely modulated zones (often masked to “zero”). While considered unreliable for reasons stated above, the equation to estimate SNR of an ROI in signal-producing region relative to background region is:

1281

1282

1283

1284

1285

1286

1287

1288

$$SNR_{vs\ bkgnd} = \frac{\text{Spatial mean pixel value on Signal Image}}{\text{Spatial standard deviation pixel value in background ROI}} \quad \text{EQ(8)}$$

1289

Since performed on magnitude images, this procedure under-estimates noise thus over-estimates SNR. This Rician bias may be predicted using DWI DRO and could be appropriately factored into further analysis of ADC statistics [92, 93, 116].

1290

1291

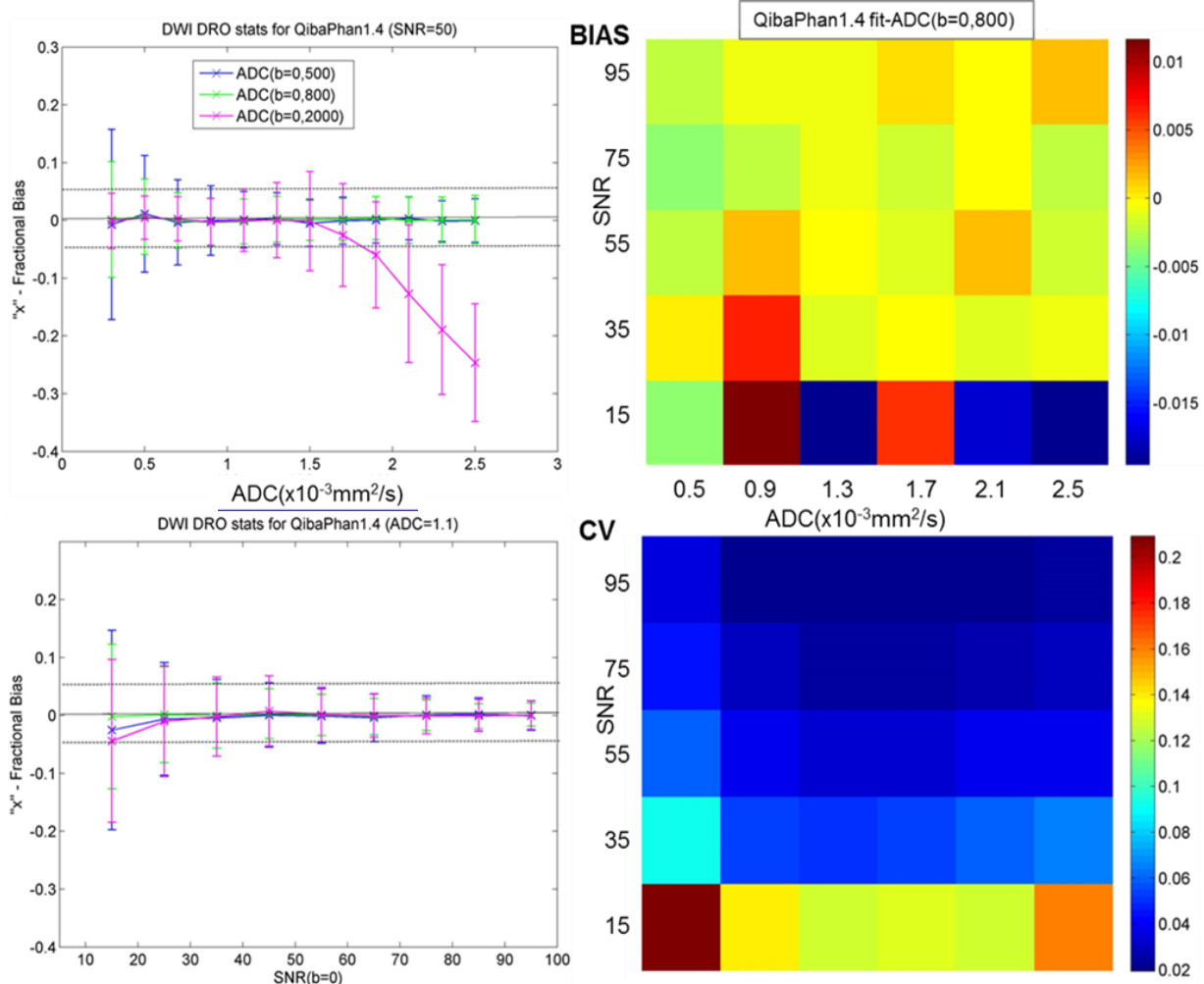


Figure E.1: Examples of fractional-bias and CV metrics for DWI-DRO ADC maps generated using QibaPhan1.4 SW. Left panes show fractional ADC bias and SD (error-bars) as a function of true (i.e., DRO input) ADC (top: at SNR=50) and SNR (bottom: at ADC=1.1 x10⁻³mm²/s) for three b-values (color-coded in legend). The dotted horizontal lines mark ±5% deviation to guide optimal DWI parameter ranges for ADC, SNR, b-value. Mean bias appears to be dependent on ADC and b-value and independent of SNR, while bias SD closely follows CV-trend and mostly SNR-dependent. Right panes show the SNR/ADC maps for mean bias and CV metrics at b-value=800 (typical of liver DWI protocol), indicating that the fit-ADC bias error (mean +/- SD) falls within +/-5% for SNR>50 in liver ADC range (0.7-1.7)x10⁻³mm²/s.

1292

1293 At a minimum, the evaluation procedure outlined in EQ(6) and EQ(7) should be performed on the $b=0$
 1294 diffusion weighted image. Low SNR conditions can introduce bias in ADC measurement (see Figure E.1).
 1295 To satisfy site qualification requirements (3.2.2) and avoid introduction of bias due to low SNR conditions,
 1296 an MRI system should have $SNR \geq 50 \pm 5$ for the $b=0$ image in an ROI of 1 cm diameter (80-100 pixels).
 1297 This SNR will allow measurement of mono-exponential diffusion media having diffusion coefficients \leq
 1298 $1.1 \times 10^{-3} \text{ mm}^2/\text{s}$ (e.g., water at 0 °C) using b -values $\leq 2000 \text{ s}/\text{mm}^2$ and avoid incremental bias due to noise.
 1299 SNR limits for different ADC and b -value ranges relevant for clinical trials should be assessed using the
 1300 DWI DRO provided through the QIDW (e.g., Figure E.1).

1301

E.3. ADC B-VALUE DEPENDENCE

1302

1303 The QIBA DWI phantom and other ice water phantoms *should* exhibit mono-exponential signal decay with
 1304 increasing b -value. Any apparent change in measured ADC with choice of b -value suggests one or
 1305 combination of the following: (1) output gradient amplitude is not linear with input demand; (2) background
 gradients that have substantial but variable contribution to the actual b -value; (3) spurious signal in $b \approx 0$

DWI that is eliminated at moderately low b -values (e.g., $b \geq 50$ s/mm²); and (4) inadequate SNR at high b -values. To evaluate whether an MRI system exhibits artefactual b -value dependence in ADC measurement, ADC values measured at isocenter on an ice water phantom should be compared as a function of b -value pairs described in equation 1. The lowest b -value (typically $b_{min} = 0$) must be included in each b -value pair. The assessor should calculate b -value dependence as:

$$ADC \text{ bvalue dependence} = 100\% \left\| \left\| \frac{(ADC_{b_{min},b_2} - ADC_{b_{min},b_1})}{ADC_{b_{min},b_1}} \right\| \right\|, \quad \text{EQ(9)}$$

where $b_2 \neq b_1$. Note, adequate diffusion contrast is required for ADC estimation via EQ(1), therefore both $(b_1 - b_{min})$ and $(b_2 - b_{min})$ should be ≥ 400 s/mm². The allowed b -value dependence that would not influence significantly the claims of this profile, is $< 2\%$ (3.2.2).

In the absence of a phantom with varying ADC with known ground truths, this b -value dependence assessment provides a suitable test for ADC linearity.

E.4. ADC SPATIAL DEPENDENCE

All ADC calculations described above utilize nominal b -values entered by the assessor during DWI acquisition and retained in DICOM headers. In turn, b -value selection determines amplitude and timing of diffusion-encoding gradient pulses within the diffusion sequence. Due to current physical constraints of gradient designs, gradient strength is not spatially uniform throughout the imaged volume. The greatest contributor to spatial ADC bias is gradient nonlinearity, although other sources such as uniformity of the main magnetic field can also contribute to spatial ADC bias at off-center locations [61, 65, 119-123]. Regardless of source, the maximum level of allowable spatial ADC bias of an MRI system depends on scale of the imaging volume for the specific clinical application. For example, DWI studies dedicated to the prostate or brain lesions could benefit from relatively minimal expected spatial ADC bias when the imaging prescription requires the lesion be located near superior/inferior = 0 mm; whereas bilateral breast or unilateral off-center liver DWI will likely experience greater spatial ADC bias. For MRI system performance evaluation, a DWI phantom should be selected that reasonably spans the imaging volume of the associated clinical application and that preferably fits in the same application-specific receiver coil. By its physical nature (determined by gradient coil design), spatial ADC bias is expected to be independent of b -value and ADC range. Thus, assessment of this bias for phantom is a reasonable estimate for bias in patient scans in clinical trials. In the context of clinical trial, spatial ADC bias is expected to increase both the ROI ADC error (i.e., in ROI mean and ADC histogram width, and increasing wCV), and the variability among systems.

Using DWI phantom with known diffusion coefficient, such as the QIBA DWI phantom or other suitable ice water-based phantom, the site should follow established phantom preparation instructions, and acquire DWI using a protocol matched to the associated application. Using EQ(2), ADC bias should be measured from multiple ROIs containing at least 80 pixels each that reasonably sample spatial offset(s) from magnet isocenter anticipated for the specific clinical application. Maximum allowed bias for a system qualified for this profile (3.2.2) will increase with maximum allowed offset from isocenter (4% for 4 cm AP/RL/SI, 10% for RL/AP < 10 cm (SI < 4 cm) or SI < 5 cm (RL/AP < 4 cm)).

1346 **Appendix F: Checklists**

1347 **F.1. SITE CHECKLIST**

1348

Parameter	Conforms (Y/N)	Requirement	Site Opinion
Site Qualification (Section 3.2)			
Qualification activities	<input type="checkbox"/> Yes <input type="checkbox"/> No	Shall perform qualification activities for Acquisition Device, Scanner Operator, and Image Analyst to meet equipment, reconstruction SW, image analysis tool and phantom ADC performance metrics as specified in Table 3.2.2 and by trial-specific protocol 3.6.2	<input type="checkbox"/> Routinely do already <input type="checkbox"/> Feasible, will do <input type="checkbox"/> Feasible, will not do <input type="checkbox"/> Not feasible (explain why)
Periodic QA (Section 3.5)			
Periodic DWI QA	<input type="checkbox"/> Yes <input type="checkbox"/> No	Shall perform periodic QA for Acquisition Device that includes assessment of ADC bias, random error, linearity, DWI SNR, DWI image artefacts, <i>b</i> -value dependence (linearity) and spatial uniformity (3.2.2)	<input type="checkbox"/> Routinely do already <input type="checkbox"/> Feasible, will do <input type="checkbox"/> Feasible, will not do <input type="checkbox"/> Not feasible (explain why)
Equipment	<input type="checkbox"/> Yes <input type="checkbox"/> No	Same, pre-qualified equipment and SW shall be used over the length of trial, and all preventive maintenance shall be documented over the course of the trial. Re-qualification shall be performed in case of major SW or hardware upgrade.	<input type="checkbox"/> Routinely do already <input type="checkbox"/> Feasible, will do <input type="checkbox"/> Feasible, will not do <input type="checkbox"/> Not feasible (explain why)

1349

1350

1351
1352

F.2. ACQUISITION DEVICE CHECKLIST

Parameter	Conforms (Y/N)	Requirement	Site Opinion
Site Qualification (Section 3.2)			
Acquisition Protocols	<input type="checkbox"/> Yes <input type="checkbox"/> No	Shall be capable of storing protocols and performing scans with all the parameters set as specified in Section 3.6 "Protocol Design Specification" and Appendix D	<input type="checkbox"/> Routinely do already <input type="checkbox"/> Feasible, will do <input type="checkbox"/> Feasible, will not do <input type="checkbox"/> Not feasible (explain why)
DWI Tags	<input type="checkbox"/> Yes <input type="checkbox"/> No	Shall preserve tags related to DWI, including private tags, which may be vendor-specific. Some key tags are specified in Appendix D.	<input type="checkbox"/> Routinely do already <input type="checkbox"/> Feasible, will do <input type="checkbox"/> Feasible, will not do <input type="checkbox"/> Not feasible (explain why)
Short-term (intra-exam) ADC repeatability at/near isocenter	<input type="checkbox"/> Yes <input type="checkbox"/> No	$RC \leq 1.5 \times 10^{-5} \text{ mm}^2/\text{s}$ and $wCV \leq 0.5\%$ for ice-water phantom or other quantitative DWI phantom	<input type="checkbox"/> Routinely do already <input type="checkbox"/> Feasible, will do <input type="checkbox"/> Feasible, will not do <input type="checkbox"/> Not feasible (explain why)
Long-term (multi-day) ADC repeatability at/near isocenter	<input type="checkbox"/> Yes <input type="checkbox"/> No	$RC \leq 6.5 \times 10^{-5} \text{ mm}^2/\text{s}$ and $wCV \leq 2.2\%$ for ice-water phantom or other quantitative DWI phantom	<input type="checkbox"/> Routinely do already <input type="checkbox"/> Feasible, will do <input type="checkbox"/> Feasible, will not do <input type="checkbox"/> Not feasible (explain why)
DWI $b=0$ SNR	<input type="checkbox"/> Yes <input type="checkbox"/> No	$SNR (b=0) \geq 50 \pm 5$ for ice-water phantom or other quantitative DWI phantom.	<input type="checkbox"/> Routinely do already <input type="checkbox"/> Feasible, will do <input type="checkbox"/> Feasible, will not do <input type="checkbox"/> Not feasible (explain why)
ADC b -value dependence	<input type="checkbox"/> Yes <input type="checkbox"/> No	$< 2\%$ for ice-water phantom or other quantitative DWI phantom over b -value pairs 0-500; 0-900; and 0-2000 s/mm^2	<input type="checkbox"/> Routinely do already <input type="checkbox"/> Feasible, will do <input type="checkbox"/> Feasible, will not do <input type="checkbox"/> Not feasible (explain why)
Maximum bias with offset from isocenter: within 4 cm in any direction	<input type="checkbox"/> Yes <input type="checkbox"/> No	$< 4\%$ for uniform DWI phantom	<input type="checkbox"/> Routinely do already <input type="checkbox"/> Feasible, will do <input type="checkbox"/> Feasible, will not do <input type="checkbox"/> Not feasible (explain why)
R/L offset < 10 cm (with A/P and S/I < 4 cm)	<input type="checkbox"/> Yes <input type="checkbox"/> No	$< 10\%$ for uniform DWI phantom	<input type="checkbox"/> Routinely do already <input type="checkbox"/> Feasible, will do <input type="checkbox"/> Feasible, will not do <input type="checkbox"/> Not feasible (explain why)
A/P offset < 10 cm (with R/L and S/I < 4 cm)	<input type="checkbox"/> Yes <input type="checkbox"/> No	$< 10\%$ for uniform DWI phantom	<input type="checkbox"/> Routinely do already <input type="checkbox"/> Feasible, will do <input type="checkbox"/> Feasible, will not do <input type="checkbox"/> Not feasible (explain why)

Parameter	Conforms (Y/N)	Requirement	Site Opinion
S/I offset < 5 cm (with R/L and A/P < 4 cm)	<input type="checkbox"/> Yes <input type="checkbox"/> No	< 10% for uniform DWI phantom	<input type="checkbox"/> Routinely do already <input type="checkbox"/> Feasible, will do <input type="checkbox"/> Feasible, will not do <input type="checkbox"/> Not feasible (explain why)
Pre-delivery (Section 3.3)			
Performance metrics	<input type="checkbox"/> Yes <input type="checkbox"/> No	Scanner shall meet established vendor performance metrics for given model	<input type="checkbox"/> Routinely do already <input type="checkbox"/> Feasible, will do <input type="checkbox"/> Feasible, will not do <input type="checkbox"/> Not feasible (explain why)
DWI sequence	<input type="checkbox"/> Yes <input type="checkbox"/> No	Scanner shall be capable to acquire single-shot DWI	<input type="checkbox"/> Routinely do already <input type="checkbox"/> Feasible, will do <input type="checkbox"/> Feasible, will not do <input type="checkbox"/> Not feasible (explain why)
DICOM conformance	<input type="checkbox"/> Yes <input type="checkbox"/> No	Shall be capable of performing reconstructions and producing images with all the parameters set as specified in 3.4.2 "Protocol Design Specification".	<input type="checkbox"/> Routinely do already <input type="checkbox"/> Feasible, will do <input type="checkbox"/> Feasible, will not do <input type="checkbox"/> Not feasible (explain why)
Periodic QA (Section 3.5)			
Periodic DWI QA	<input type="checkbox"/> Yes <input type="checkbox"/> No	Shall perform system qualification and periodic QA that includes assessment of ADC bias, random error, linearity, DWI SNR, DWI image artefacts, <i>b</i> -value dependence and spatial uniformity (3.2)	<input type="checkbox"/> Routinely do already <input type="checkbox"/> Feasible, will do <input type="checkbox"/> Feasible, will not do <input type="checkbox"/> Not feasible (explain why)
Protocol Design (Section 3.6)			
Scan Protocol Parameters	<input type="checkbox"/> Yes <input type="checkbox"/> No	Device scan protocol parameters shall be within organ-specific ranges listed in the protocol specification tables (3.6.2)	<input type="checkbox"/> Routinely do already <input type="checkbox"/> Feasible, will do <input type="checkbox"/> Feasible, will not do <input type="checkbox"/> Not feasible (explain why)
Image Data Acquisition (Section 3.9)			
Scan Procedure	<input type="checkbox"/> Yes <input type="checkbox"/> No	Study of each patient shall be performed on the site pre-qualified scanner using approved receiver coil and pre-built profile-conformant scan protocol (3.6).	<input type="checkbox"/> Routinely do already <input type="checkbox"/> Feasible, will do <input type="checkbox"/> Feasible, will not do <input type="checkbox"/> Not feasible (explain why)

1354
1355
1356

F.3. SCANNER OPERATOR CHECKLIST

Parameter	Conforms (Y/N)	Requirement	Site Opinion
Site Qualification (section 3.2)			
Acquisition Protocols	<input type="checkbox"/> Yes <input type="checkbox"/> No	Shall prepare scan protocols conformant with section 3.6.2 "Protocol Design Specification" and phantom qualification (Appendix D) and ensure that DWI acquisition parameters (<i>b</i> -value, diffusion direction) shall be preserved in DICOM and shall be within ranges allowed by study protocol (both for phantom and subject scans).	<input type="checkbox"/> Routinely do already <input type="checkbox"/> Feasible, will do <input type="checkbox"/> Feasible, will not do <input type="checkbox"/> Not feasible (explain why)
Acquisition Device Performance	<input type="checkbox"/> Yes <input type="checkbox"/> No	Shall perform assessment procedures (Section 4) for site qualification and longitudinal QA for the acquisition devices participating in trial to document acceptable performance for phantom ADC metrics as specified in table 3.2.2	<input type="checkbox"/> Routinely do already <input type="checkbox"/> Feasible, will do <input type="checkbox"/> Feasible, will not do <input type="checkbox"/> Not feasible (explain why)
Reconstruction SW Performance	<input type="checkbox"/> Yes <input type="checkbox"/> No	Shall confirm that reconstruction SW is capable of performing reconstructions and producing images with all the parameters set as specified in section 3.6.2 "Protocol Design Specification" and meet DWI DICOM header and image registration requirements specified in 3.10.2, including storage of <i>b</i> -values, DWI directionality, image scaling and units tags, as specified in DICOM conformance statement for the given scanner SW version, as well as the model-specific Reconstruction Software parameters utilized to achieve conformance.	<input type="checkbox"/> Routinely do already <input type="checkbox"/> Feasible, will do <input type="checkbox"/> Feasible, will not do <input type="checkbox"/> Not feasible (explain why)
Periodic QA (section 3.5)			
Periodic DWI QA	<input type="checkbox"/> Yes <input type="checkbox"/> No	Shall perform system qualification and periodic QA that includes assessment of ADC bias, random error, linearity, DWI SNR, DWI image artefacts, <i>b</i> -value dependence and spatial uniformity (3.2.2)	<input type="checkbox"/> Routinely do already <input type="checkbox"/> Feasible, will do <input type="checkbox"/> Feasible, will not do <input type="checkbox"/> Not feasible (explain why)
Protocol Design (section 3.6)			
Protocol	<input type="checkbox"/> Yes <input type="checkbox"/> No	Shall check that implemented scan protocol parameters comply with the organ-specific scan protocol requirements as detailed in the profile specifications in Table 3.6.2.	<input type="checkbox"/> Routinely do already <input type="checkbox"/> Feasible, will do <input type="checkbox"/> Feasible, will not do <input type="checkbox"/> Not feasible (explain why)

Parameter	Conforms (Y/N)	Requirement	Site Opinion
Image Data Acquisition (section 3.9)			
Patient Positioning	<input type="checkbox"/> Yes <input type="checkbox"/> No	Predefined positioning procedure and receiver coil (e.g., always head-first or always feet-first, torso phased-array) shall be used for all study subjects. Subject-specific landmark shall be centered on the target organ, which shall be located as close as is feasible to magnet isocenter.	<input type="checkbox"/> Routinely do already <input type="checkbox"/> Feasible, will do <input type="checkbox"/> Feasible, will not do <input type="checkbox"/> Not feasible (explain why)
Scan Parameters	<input type="checkbox"/> Yes <input type="checkbox"/> No	Subject-specific adjustments within allowed parameter ranges (Table 3.6.2) shall be made to suit body habitus. Parameter adjustments for a given subject shall be constant for serial scans.†	<input type="checkbox"/> Routinely do already <input type="checkbox"/> Feasible, will do <input type="checkbox"/> Feasible, will not do <input type="checkbox"/> Not feasible (explain why)
Acquisition Device	<input type="checkbox"/> Yes <input type="checkbox"/> No	The same scanner shall be used for baseline measurement and a subsequent longitudinal measurement for detecting change in ADC.	<input type="checkbox"/> Routinely do already <input type="checkbox"/> Feasible, will do <input type="checkbox"/> Feasible, will not do <input type="checkbox"/> Not feasible (explain why)
Image Data Reconstruction (section 3.10)			
Trace DWI and ADC map generation across subjects and time	<input type="checkbox"/> Yes <input type="checkbox"/> No	Procedural steps for image reconstruction, archiving of original, uncorrected images (if generated), and ADC map generation shall be held constant for all subjects and time points including: image interpolation; image registration prior to combination into trace DWI and across <i>b</i> -values; selection of <i>b</i> -values and fit algorithm to estimate ADC. ADC shall be calculated using the mono-exponential model of DWI signal decay with increasing <i>b</i> -value, starting with protocol-specific low <i>b</i> -value to compensate for perfusion effects.	<input type="checkbox"/> Routinely do already <input type="checkbox"/> Feasible, will do <input type="checkbox"/> Feasible, will not do <input type="checkbox"/> Not feasible (explain why)
<i>b</i> -value record	<input type="checkbox"/> Yes <input type="checkbox"/> No	Scanner operator shall verify that the reconstruction SW records <i>b</i> -values, or if not shall manually record the <i>b</i> -values, that are used to generate the ADC map.	<input type="checkbox"/> Routinely do already <input type="checkbox"/> Feasible, will do <input type="checkbox"/> Feasible, will not do <input type="checkbox"/> Not feasible (explain why)
Image QA (section 3.11)			
ADC quality	<input type="checkbox"/> Yes <input type="checkbox"/> No	Shall confirm DWI and ADC maps conform to adequate quality specifically considering points listed above (3.11.1) and shall exclude artefact-rich images and ROI from repeatability analysis.	<input type="checkbox"/> Routinely do already <input type="checkbox"/> Feasible, will do <input type="checkbox"/> Feasible, will not do <input type="checkbox"/> Not feasible (explain why)
Image Distribution (section 3.12)			

Parameter	Conforms (Y/N)	Requirement	Site Opinion
Trace DWI	<input type="checkbox"/> Yes <input type="checkbox"/> No	All trace DWI at each acquired <i>b</i> -value shall be stored in local PACS and distributed to image analysis workstation(s)	<input type="checkbox"/> Routinely do already <input type="checkbox"/> Feasible, will do <input type="checkbox"/> Feasible, will not do <input type="checkbox"/> Not feasible (explain why)
ADC maps	<input type="checkbox"/> Yes <input type="checkbox"/> No	ADC maps generated on the MRI scanner shall be stored in local PACS and distributed to image analysis workstation(s) with preserved DICOM scale tags. ADC map scale/units and <i>b</i> -values used for generation shall be recorded.	<input type="checkbox"/> Routinely do already <input type="checkbox"/> Feasible, will do <input type="checkbox"/> Feasible, will not do <input type="checkbox"/> Not feasible (explain why)
Image DICOM	<input type="checkbox"/> Yes <input type="checkbox"/> No	DICOM tags essential for downstream review and diffusion analysis shall be maintained including, pixel intensity scaling [113], <i>b</i> -value, and DWI directionality vs. trace, and ADC scale and units. Trace DWI DICOM at each acquired <i>b</i> -value shall be archived in the local PACS.	<input type="checkbox"/> Routinely do already <input type="checkbox"/> Feasible, will do <input type="checkbox"/> Feasible, will not do <input type="checkbox"/> Not feasible (explain why)

1358
1359
1360

F.4. IMAGE ANALYST CHECKLIST

Parameter	Conforms (Y/N)	Requirement	Site Opinion
Staff Qualification (section 3.1)			
Qualification	<input type="checkbox"/> Yes <input type="checkbox"/> No	May be a radiologist, technologist, physicist, or other scientist that shall undergo documented training by a qualified radiologist in terms of anatomical location and image contrast(s) used to select measurement target; and by qualified physicist in understanding key DWI acquisition principles of diffusion weighting and directionality and diffusion test procedures, procedures to confirm that diffusion-related DICOM metadata content is maintained along the network chain from Scanner to PACS and analysis workstation and in use of the Image Analysis Tool, including ADC map generation from DWI (if not generated on the scanner), and ADC map reduction to statistics with ROI/VOI location(s)	<input type="checkbox"/> Routinely do already <input type="checkbox"/> Feasible, will do <input type="checkbox"/> Feasible, will not do <input type="checkbox"/> Not feasible (explain why)
Site Qualification (section 3.2)			
Image Analysis Tool Performance	<input type="checkbox"/> Yes <input type="checkbox"/> No	Shall test Image Analysis Tool to ensure acceptable performance according to 3.13.2 specifications for study image visualization, DICOM and analysis meta-data interpretation and storage, ROI segmentation, and generation of ADC maps and repeatability statistics for qualification phantom (below)	<input type="checkbox"/> Routinely do already <input type="checkbox"/> Feasible, will do <input type="checkbox"/> Feasible, will not do <input type="checkbox"/> Not feasible (explain why)
Phantom ADC ROI	<input type="checkbox"/> Yes <input type="checkbox"/> No	Shall confirm that phantom ADC ROI is 1-2 cm diameter (>80 pixels without interpolation) for all Acquisition Device specifications in Table 3.2.2	<input type="checkbox"/> Routinely do already <input type="checkbox"/> Feasible, will do <input type="checkbox"/> Feasible, will not do <input type="checkbox"/> Not feasible (explain why)
Phantom ADC metrics	<input type="checkbox"/> Yes <input type="checkbox"/> No	Shall evaluate and record phantom ADC metrics (bias, linearity and precision) according to Table 3.2.2 specifications for Acquisition Device qualification and periodic QA using QIBA-provided or qualified site Image Analysis Tool	<input type="checkbox"/> Routinely do already <input type="checkbox"/> Feasible, will do <input type="checkbox"/> Feasible, will not do <input type="checkbox"/> Not feasible (explain why)
Image QA (section 3.11)			
ADC quality		Shall confirm DWI and ADC maps conform to adequate quality specifically	<input type="checkbox"/> Routinely do already <input type="checkbox"/> Feasible, will do

Parameter	Conforms (Y/N)	Requirement	Site Opinion
	<input type="checkbox"/> Yes <input type="checkbox"/> No	considering points listed above (3.11.1) and shall exclude artefact-rich images and ROI from repeatability analysis.	<input type="checkbox"/> Feasible, will not do <input type="checkbox"/> Not feasible (explain why)
Image Distribution (section 3.12)			
Trace DWI	<input type="checkbox"/> Yes <input type="checkbox"/> No	Shall ensure that all trace DWI at each acquired <i>b</i> -value shall be stored in local PACS and distributed to image analysis workstation(s)	<input type="checkbox"/> Routinely do already <input type="checkbox"/> Feasible, will do <input type="checkbox"/> Feasible, will not do <input type="checkbox"/> Not feasible (explain why)
ADC maps	<input type="checkbox"/> Yes <input type="checkbox"/> No	ADC maps generated on the MRI scanner shall be stored in local PACS and distributed to image analysis workstation(s) with preserved DICOM scale tags. ADC map scale/units and <i>b</i> -values used for generation shall be recorded.	<input type="checkbox"/> Routinely do already <input type="checkbox"/> Feasible, will do <input type="checkbox"/> Feasible, will not do <input type="checkbox"/> Not feasible (explain why)
Image DICOM	<input type="checkbox"/> Yes <input type="checkbox"/> No	DICOM tags essential for downstream review and diffusion analysis shall be maintained including, pixel intensity scaling [113], <i>b</i> -value, and DWI directionality vs. trace, and ADC scale and units. Trace DWI DICOM at each acquired <i>b</i> -value shall be archived in the local PACS.	<input type="checkbox"/> Routinely do already <input type="checkbox"/> Feasible, will do <input type="checkbox"/> Feasible, will not do <input type="checkbox"/> Not feasible (explain why)
Image Analysis (section 3.13)			
ROI Determination	<input type="checkbox"/> Yes <input type="checkbox"/> No	Shall segment the ROI on ADC maps consistently across time points using the same software / analysis package guided by a fixed set of image contrasts and avoiding artefacts	<input type="checkbox"/> Routinely do already <input type="checkbox"/> Feasible, will do <input type="checkbox"/> Feasible, will not do <input type="checkbox"/> Not feasible (explain why)

1361
1362

1363

F.5. RECONSTRUCTION SOFTWARE

1364

Image Data Reconstruction (Section 3.10)			
Trace DWI	<input type="checkbox"/> Yes <input type="checkbox"/> No	Trace DWI shall be auto-generated on the scanner and retained for all $b > 0$. For equal b -value on 3 orthogonal directions, trace DWI is the geometric average of the 3-orthogonal directional DWI.	<input type="checkbox"/> Routinely do already <input type="checkbox"/> Feasible, will do <input type="checkbox"/> Feasible, will not do <input type="checkbox"/> Not feasible (explain why)
DICOM DWI	<input type="checkbox"/> Yes <input type="checkbox"/> No	Exported DWI DICOM shall provide acquired b -values and directionality.	<input type="checkbox"/> Routinely do already <input type="checkbox"/> Feasible, will do <input type="checkbox"/> Feasible, will not do <input type="checkbox"/> Not feasible (explain why)
Spatial Registration	<input type="checkbox"/> Yes <input type="checkbox"/> No	Spatial misalignment between directional DWI and across b -values due to eddy currents or patient motion shall be corrected by image registration prior to generation of trace DWI and ADC maps.	<input type="checkbox"/> Routinely do already <input type="checkbox"/> Feasible, will do <input type="checkbox"/> Feasible, will not do <input type="checkbox"/> Not feasible (explain why)

1365

1366

1367
1368
1369

F.6. IMAGE ANALYSIS TOOL CHECKLIST

ACCEPTABLE: Actors that shall meet this specification to conform to this profile.

TARGET: Meeting this specification is achievable with reasonable effort and adequate equipment and is expected to provide better results than meeting the ACCEPTABLE specification.

IDEAL: Meeting this specification may require extra effort or non-standard hardware or software, but is expected to provide better results than meeting the TARGET.

Parameter	Conforms (Y/N)	Requirement	Site Opinion
Image Analysis (section 3.13)			
ROI geometry	<input type="checkbox"/> Yes <input type="checkbox"/> No	Acceptable: Screen-shot(s) documenting ROI placement on ADC maps shall be retained in the subject database for future reference Target: ROI as a binary pixel mask in image coordinates shall be retained in the subject database for future reference Ideal: ROI shall be saved as a DICOM segment object	<input type="checkbox"/> Routinely do already <input type="checkbox"/> Feasible, will do <input type="checkbox"/> Feasible, will not do <input type="checkbox"/> Not feasible (explain why)
Image Display	<input type="checkbox"/> Yes <input type="checkbox"/> No	Acceptable / Target: Software shall allow operator-defined ROI analysis of DWI/ADC aided by inspection of ancillary MR contrasts Ideal: Above plus multi view-port display where DWI/ADC and ancillary MR contrasts from the same scan date are displayed side-by-side and geometrically linked per DICOM (e.g., cursor; cross-hair; ROI; automatically replicated in all view-ports); images from different scan date(s) can be displayed side-by-side, though not necessarily geometrically linked; and ROIs/VOIs may include multiple noncontiguous areas on one slice and/or over multiple slices	<input type="checkbox"/> Routinely do already <input type="checkbox"/> Feasible, will do <input type="checkbox"/> Feasible, will not do <input type="checkbox"/> Not feasible (explain why)
Analysis Procedure	<input type="checkbox"/> Yes <input type="checkbox"/> No	Analysis steps, derived metrics and analysis software package shall be held constant for all subjects and serial time points	<input type="checkbox"/> Routinely do already <input type="checkbox"/> Feasible, will do <input type="checkbox"/> Feasible, will not do <input type="checkbox"/> Not feasible (explain why)
ADC statistics		Acceptable/Target: Shall allow display and retention of ROI statistics in patient	<input type="checkbox"/> Routinely do already

Parameter	Conforms (Y/N)	Requirement	Site Opinion
	<input type="checkbox"/> Yes <input type="checkbox"/> No	DICOM database (PACS). Statistics shall include: ADC mean, standard deviation, and ROI/VOI area/volume Ideal: ADC pixel histogram, additional statistics for ADC maximum, minimum, explicit inclusion vs. exclusion of “NaNs” or zero-valued pixels shall be retained with the statistics	<input type="checkbox"/> Feasible, will do <input type="checkbox"/> Feasible, will not do <input type="checkbox"/> Not feasible (explain why)
ADC scaling	<input type="checkbox"/> Yes <input type="checkbox"/> No	ADC maps scale and units shall be recorded. The difference(s) in mean ADC within replicate ROIs defined on the scanner and analysis workstation(s) shall be less than the ROI standard deviation of the ADC.	<input type="checkbox"/> Routinely do already <input type="checkbox"/> Feasible, will do <input type="checkbox"/> Feasible, will not do <input type="checkbox"/> Not feasible (explain why)
ADC map storage	<input type="checkbox"/> Yes <input type="checkbox"/> No	Acceptable/Target: offline generated ADC maps shall be stored in ITK-compatible format (e.g., NIFTI or MHD) with meta-data traceable to original DWI DICOM (and geometry) Ideal: parametric map DICOM)	<input type="checkbox"/> Routinely do already <input type="checkbox"/> Feasible, will do <input type="checkbox"/> Feasible, will not do <input type="checkbox"/> Not feasible (explain why)
Fit algorithm type	<input type="checkbox"/> Yes <input type="checkbox"/> No	The specific choice of the fit algorithm shall be recorded, held constant within a study and reported with any dissemination of study findings.	<input type="checkbox"/> Routinely do already <input type="checkbox"/> Feasible, will do <input type="checkbox"/> Feasible, will not do <input type="checkbox"/> Not feasible (explain why)
Fit algorithm bias	<input type="checkbox"/> Yes <input type="checkbox"/> No	For offline ADC map generation, the mean ADC shall agree with scanner-generated, or DRO ground truth, ADC values to within one ROI standard deviation.	<input type="checkbox"/> Routinely do already <input type="checkbox"/> Feasible, will do <input type="checkbox"/> Feasible, will not do <input type="checkbox"/> Not feasible (explain why)
<i>b</i> -value and direction	<input type="checkbox"/> Yes <input type="checkbox"/> No	Software shall extract <i>b</i> -values and diffusion axis direction from DICOM header	<input type="checkbox"/> Routinely do already <input type="checkbox"/> Feasible, will do <input type="checkbox"/> Feasible, will not do <input type="checkbox"/> Not feasible (explain why)